

## Dam-induced hydrological alterations in the upper Cauvery river basin, India

Ekka, Anjana; Keshav, Saket; Pande, Saket; van der Zaag, Pieter; Jiang, Yong

**DOI**

[10.1016/j.ejrh.2022.101231](https://doi.org/10.1016/j.ejrh.2022.101231)

**Publication date**

2022

**Document Version**

Final published version

**Published in**

Journal of Hydrology: Regional Studies

**Citation (APA)**

Ekka, A., Keshav, S., Pande, S., van der Zaag, P., & Jiang, Y. (2022). Dam-induced hydrological alterations in the upper Cauvery river basin, India. *Journal of Hydrology: Regional Studies*, 44, Article 101231. <https://doi.org/10.1016/j.ejrh.2022.101231>

**Important note**

To cite this publication, please use the final published version (if applicable). Please check the document version above.

**Copyright**

Other than for strictly personal use, it is not permitted to download, forward or distribute the text or part of it, without the consent of the author(s) and/or copyright holder(s), unless the work is under an open content license such as Creative Commons.

**Takedown policy**

Please contact us and provide details if you believe this document breaches copyrights. We will remove access to the work immediately and investigate your claim.



# Dam-induced hydrological alterations in the upper Cauvery river basin, India

Anjana Ekka<sup>a,c,\*</sup>, Saket Keshav<sup>a</sup>, Saket Pande<sup>a</sup>, Pieter van der Zaag<sup>a,b</sup>, Yong Jiang<sup>b</sup>

<sup>a</sup> Department of Water Management, Delft University of Technology, Delft, The Netherlands

<sup>b</sup> IHE Delft Institute for Water Education, Delft, The Netherlands

<sup>c</sup> ICAR-Central Inland Fisheries Research Institute, Barrackpore, India

## ARTICLE INFO

### Keywords:

FLEX-Topo model  
Reservoir modelling  
Indicators of hydrological alterations (IHA)  
Human water systems  
Ecosystem services  
Cauvery

## ABSTRACT

*Study region:* Upper Cauvery river basin, India

*Study focus:* Reservoir construction is one of the major contributors to changes in natural river flow regime characteristics. This study aims to understand the hydrological alterations resulting from the construction of reservoirs and water abstraction in the upper regions of the basin. The impacts of dams on river flow regimes where data is available only for periods after the construction of the dams is assessed. A landscape-based hydrological model, FLEX-Topo, is used to model the flows contributed by the upstream and downstream areas of four major reservoirs in the study area. A separate reservoir operation model is developed for each of the reservoirs. Next, the hydrological model is integrated with the reservoir model and the modelled flow at the downstream streamflow gauging station of each of the corresponding four sub-basins is calibrated. The modelled flow regimes with and without reservoirs are then compared using the indicators of hydrological alterations to understand the degree to which the flows have been altered by the reservoirs.

*New hydrological insights for the region:* The results indicate that flow regimes have been modified from their natural state following reservoir impoundment and water abstractions. Significant impacts are observed in median monthly flow, 1-day minimum flow and low pulses. Such information could provide a reference to water managers to replicate the natural flow regimes, help sustain natural biota and thus contribute toward the sustainable management of river basins in India.

## 1. Introduction

Worldwide, dams have been constructed to meet growing human needs. No doubt, dams have provided many economic benefits in the form of water supply, hydropower, and food production, which has boosted economic growth and human wellbeing. Around the world, nearly 63 per cent of the free-flowing rivers have been affected by reservoir operations, impairing the ecological functioning of the basins (Grill et al., 2019). As a result, the ecology of the dams' upstream and downstream areas is impacted (Crossman and Pollino, 2018).

The construction of a dam across a river converts a river segment of the natural watercourse into stagnant water (Gopal, 2016). This

\* Corresponding author at: Department of Water Management, Delft University of Technology, Delft, The Netherlands.  
E-mail address: [A.Ekka@tudelft.nl](mailto:A.Ekka@tudelft.nl) (A. Ekka).

changes the hydrological regime of the river in terms of magnitude, frequency, timing, duration, and rate of change in flows. Such alterations in flow regimes influence the ecological processes that impact the functioning of ecosystem services (Renofalt, 2010; Brauman et al., 2007). For example, the longitudinal and lateral connectivity is interrupted by dams and barrages resulting in fragmented biotic communities (Crook et al., 2015). The reduced flows of sediment, nutrients, and freshwater inputs into estuaries and coastal zones decrease the nutrient composition, phytoplankton composition and zooplankton diversity and impact the aquatic food web (Domingues et al., 2012; Simões et al., 2015; Van Cappellen and Maavara, 2016). Such disturbances of the aquatic food web decrease the productivity of estuarine and coastal habitats. The dams have also displaced 40–60 million people over the last 60 years (<https://www.internationalrivers.org/human-impacts-of-dams>). As a result, large dams have come under harsh criticism worldwide from environmental scientists, human rights activists, economists, and intellectuals. Large dams have gained notoriety for the detrimental environmental and social impacts that they cause, and the huge economic burden of their costs (Bhatnagar, 2004).

In India, several multipurpose dams have been constructed such as Bhakra Nangal, Nagarjunasagar, Kosi, Chambal, Hirakud, Kakrapar and Tungbhadra dams to harness water for developmental needs. These dams were built for multipurpose uses such as hydropower, irrigation, and domestic water supply and have been seen as a sign of development and economic growth (Klingensmith, 2003). According to the National Registry for Large Dams (NRLD), in 2016 a total of 4877 dams were built in India and 313 dams were still under construction. The Cauvery river is one such peninsular river that has been intensely altered by reservoirs, barrages, canals, and anicuts (masonry check dams constructed across streams to divert water) in response to rapidly growing water demands for irrigation, household consumption, and power generation (Vanham et al., 2011). While the construction of the reservoirs has helped to expand the irrigated areas in the basin, securing water availability during water stress conditions, it has aggravated water tensions due to water allocation between the upstream and downstream states (Indian semi-autonomous administrative regions through which the river runs), leading to conflicts among the states sharing the rivers (Ramaswamy, 1994; Shah, 1994; Janakarajan, 2016).

Extensive damming has also led to poor delivery of ecosystem services. Degradation in water quality is being reported extensively (Solaraj et al., 2010; Rani and Sherine, 2007). Regulating services such as sediment transport have been adversely affected, which in turn has impacted freshwater ecosystems (Vaithyanathan et al., 1992). For example, changes in aquatic species composition are being observed due to the changes in sediment loads because of the construction of the reservoirs (Venkatachalapathy and Karthikeyan, 2015; Dhanakumar et al., 2015). Moreover, the population of migratory fish species such as *Tor spp.*, *Lates calcarifer*, *Bagarius bagarius*, and *Anguilla spp* has declined due to reduced flow rates in the river (Raj, 1941).

These are some examples that underline the necessity to assess the degree to which hydrological flows are altered, i.e., deviated from the natural flows, by the construction of dams in basins such as that of Cauvery. This study is motivated by the need for a systematic assessment of hydrological alterations by the construction of major dams in the upper Cauvery basin. However, such an assessment requires sufficient hydrological data for the periods of pre and post reservoir construction, which is often not possible. The objectives of this study are therefore to i) develop and implement a robust human influenced hydrological model that can reliably simulate pre reservoir hydrological regimes and ii) deploy a systematic assessment of pre and post reservoir flow regime changes in the basin.

Many studies of dam-induced alterations have used Indicators of Hydrological Alterations (IHA) to evaluate the hydrological impacts of dams on flow regime characteristics (Gierszewski et al., 2020, 2018; Mittal et al., 2016; Song et al., 2020; do Vasco et al., 2019; Fantin-Cruz et al., 2015; Pyron et al., 2008). Before 1990, methods such as field surveys and ground photograph analyses were used to assess the impact of impoundments on river channels (Knighton, 1988). Statistical analysis including the non-parametric Mann-Kendall (MK) method (Yan et al., 2010), Pettitt's test, and flow-duration analysis (Marcinkowski and Grygoruk, 2017) were also used to contrast the flow regimes before and after hydraulic interventions. Geomorphic Change Detection (GCD) tools (<http://gcd.riverscapes.xyz/>) have also been used to qualify topographic or morphological changes after an impoundment (Wheaton, 2015). However, a more systematic assessment of flow changes is provided by the Range of Variability Approach (Richter et al., 1997) and associated with it are the Indices of Hydrological Alteration (IHA) framework (Richter et al., 1996). The IHA method takes daily streamflow values and characterizes a flow regime in terms of five ecologically significant factors: magnitude, duration, frequency, timing, and the rate of change of flows (Page et al., 2005).

Even though the IHA method provides a systematic assessment of flow changes due to hydraulic interventions, only a few studies of Indian rivers have used it. See for example the studies for the Kangsabati river (Mittal et al., 2014), the Krishna river (Kumar and Jayakumar, 2020) and the Dikrong river (Borghain et al., 2019). This paper, therefore, applies the IHA method to systematically evaluate the impacts of major dams in the upper Cauvery. However, the information on river flows, which is needed for IHA, is not available for periods before the construction of the dams. Robust hydrological modelling of basins with and without the reservoirs, which enables the analysis of how river flows are impacted by modified landscapes due to human interventions, is therefore additionally needed (Beven, 2012; O'Sullivan et al., 2019).

Different types of hydrological models have incorporated reservoir models or reservoir operations to simulate stream flows (Mateo et al., 2014; Li et al., 2019; Tehrani et al., 2021). Distributed models like DHSVM and CREST-snow have been used that combine reservoir operation modules to simultaneously assess the impacts of climate change and reservoir operations on the flow regimes (Li et al., 2019; Han et al., 2019). These models incorporate reservoir operations and are capable of taking spatial heterogeneity into account but often are data intensive in their representation of changing landscapes and the impacts on river flow regimes. For example, the SWAT model accounts for spatial heterogeneities by combining distributed data on soil, land cover and elevation and has been used to simulate hydrological regimes regulated by reservoirs at the basin scale (Sulis et al., 2009; Wang and Xia, 2010; Babur et al., 2016). In addition to the data and computational intensity of such models, if the impacts of reservoirs are to be estimated on data that is available only after the reservoirs have been constructed then another key consideration is the transferability of models in space and time (Gao et al., 2016).

Well-constrained model structures are therefore needed to perform pre-and post-reservoir assessments, especially in regions such as Cauvery where low-resolution data is often available and no records of flow regimes exist prior to the construction of the reservoirs. This motivates the use of a topography-driven rainfall-runoff model (FLEX-Topo model) which is neither computationally expensive nor data-intensive. It determines well-constrained model structures corresponding to the dominant hydrological processes in a catchment (Gao et al., 2014) that can be reliably transferred in space and time (Gao et al., 2016; Nijzink et al., 2016). The study then integrates the FLEX-Topo model with the IHA method to assess the impacts of hydrological changes due to the construction of four major dams in the upper Cauvery river basin.

The paper is organized as follows. The study area, along with reservoir details are described in the next section. The methodology that incorporates reservoir operations in a topography-driven rainfall-runoff model and its calibration are then discussed (Section 3). The results are subsequently presented (Section 4). The paper concludes with a discussion on the impacts of reservoirs on river flow regimes in the Cauvery river basin (Sections 5 and 6). The study will provide insight into sustainably managing water resources without hampering the socio-ecological integrity of the river systems.

## 2. Description of the study area

The Cauvery is one of the most critical interstate rivers of southern India, lying between longitude 75°27'E to 79°54'E and latitude 10°9'N to 13°30'N. The Cauvery basin extends over the Indian states of Tamil Nadu, Karnataka, Kerala, and the Union Territory of Puducherry, draining an area of 81,155 km<sup>2</sup> into the Bay of Bengal. Out of this, 42 per cent lies in Karnataka, 54 per cent in Tamil Nadu & Karaikkal region of Puducherry and 4 per cent in Kerala.

There are around 96 dams constructed in the Cauvery basin during the last 1000 years, out of which 70.30 per cent of dams have been used for irrigation purposes, 19.80 per cent for hydro-power generation, 6.93 per cent for both irrigation and hydropower generation, and the remaining 2.97 per cent dams are used only for drinking water supply. The Cauvery delta, Hemavathi, Mettur,

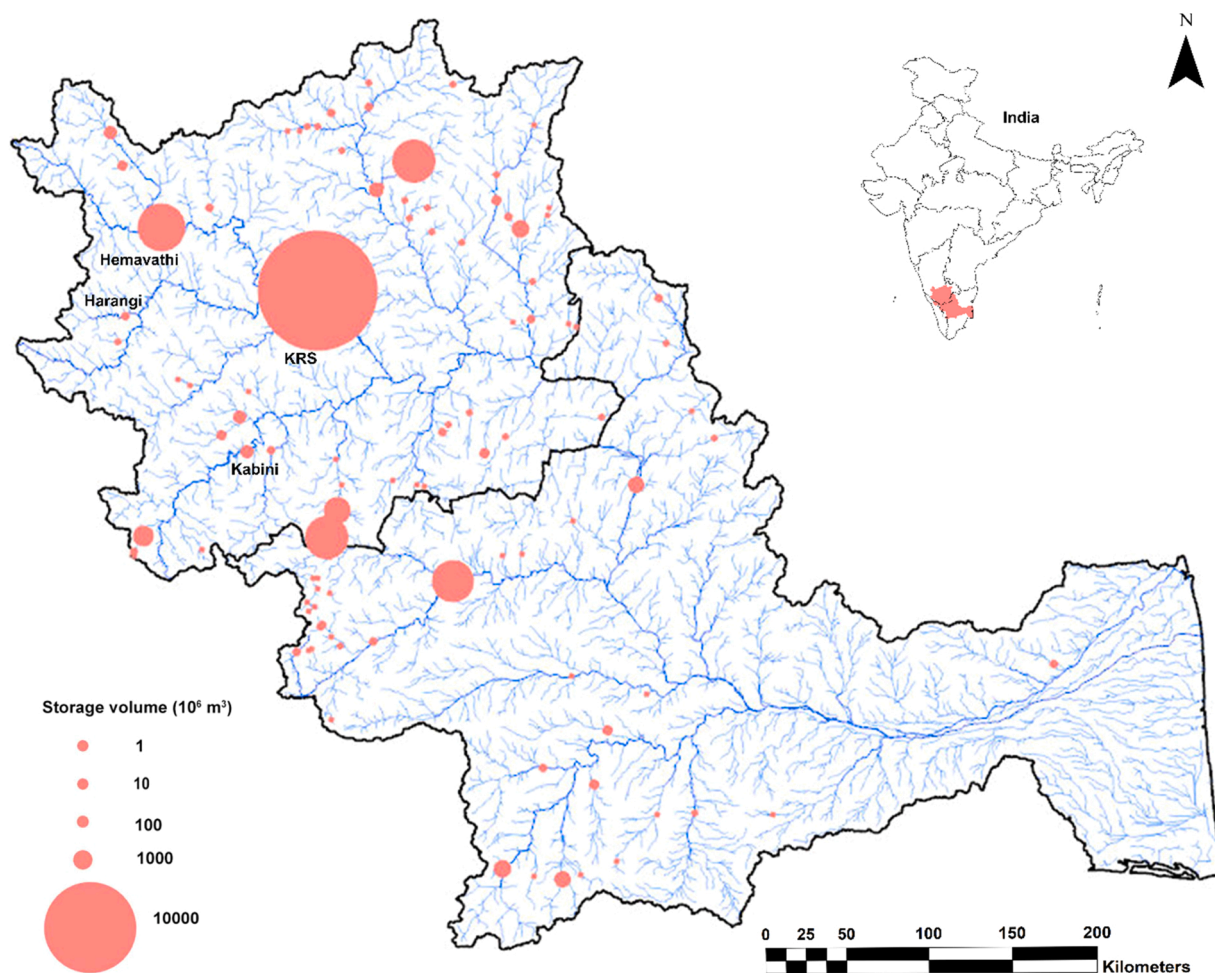


**Fig. 1.** The location of the Cauvery basin (upper Cauvery outlined) in southern India. Also shown are the relative sizes of the dams located in the Cauvery basin based on storage volume ( $10^6 \text{ m}^3$ ).

Krishna raja Sagara, and Harangi irrigation projects are among the major irrigation projects in the Cauvery basin.

As Fig. 1 shows, most of these dams are relatively small. Four major reservoirs based on size, storage capacity and command area in the upper Cauvery basin (Fig. 2) have been selected for the study. Table 1 presents a brief discussion of the reservoirs under study.

### 3. Methods

Fig. 3 illustrates the overall methodology. It involves modelling the reservoir operations, and the hydrology of areas upstream and downstream of the reservoir and then integrating the two to assess the effect of reservoirs on flow regimes observed downstream and thus on the delivery of ecosystem services. As a result, four sub-basins are studied delineated by the four gauging stations shown in Fig. 5. Each sub-basin is further sub-divided into two parts, corresponding to the areas upstream and downstream of its reservoir. Fig. 3 (b) further shows the modelling concept. F1 and F2 represent the FLEX-Topo models for upstream and downstream areas of a reservoir contributing to flow at a gauge station (GS), whereas RM and CA represent the reservoir model and associated command area respectively. The flow is measured at the downstream gauge station (GS). In the event of reservoir integration, the outflow from F1 becomes the reservoir's inflow, and the outflow from RM enters F2, after which the outflow from F2 is calibrated at GS. If the reservoir is removed, the outflow from F1 is combined with the outflow from F2, which then forms the outflow at GS.

Further, indicators of hydrological alterations, which are based on river flow characteristics, are used to understand the impact of reservoirs on the river flow regimes. The IHA method is simple to use and provides valuable information related to flow alternations and helps to assess the potential impacts that flow alterations may have on the river ecosystem.

#### 3.1. The FLEX-Topo model

Topography based landscape hydrological model, FLEX-Topo, is used (Savenije, 2010). Topography is one of the main characteristics of the river landscape, which emerges from the coevolution of vegetation and soil with climate (Savenije, 2010; Gao et al., 2014). As a result, it determines dominant hydrological processes in a catchment (Gao et al., 2014) and has been used as a strong constraint in determining and transferring the model structures in space and time (Gao et al., 2016; Nijzink et al., 2016). The model

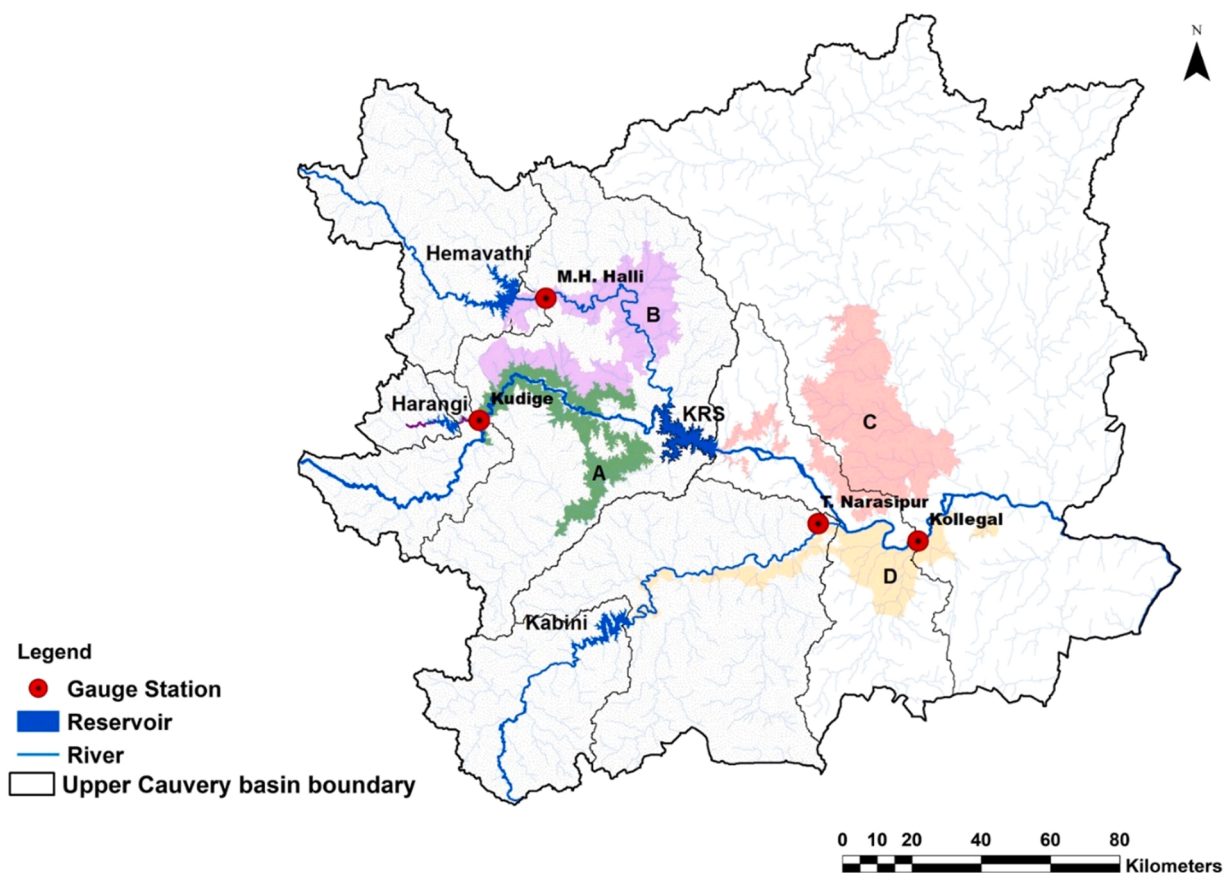
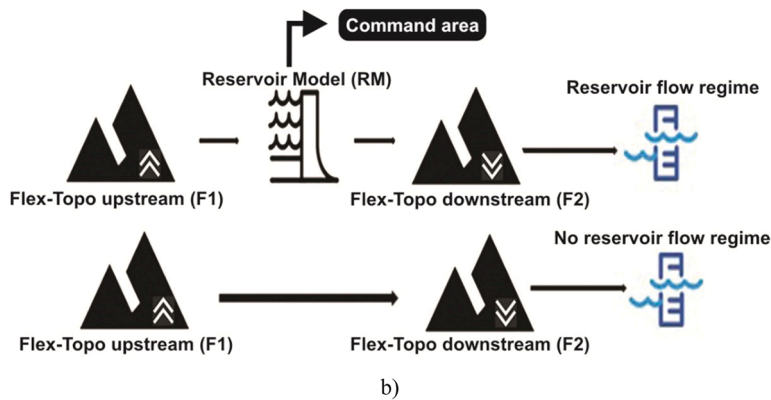
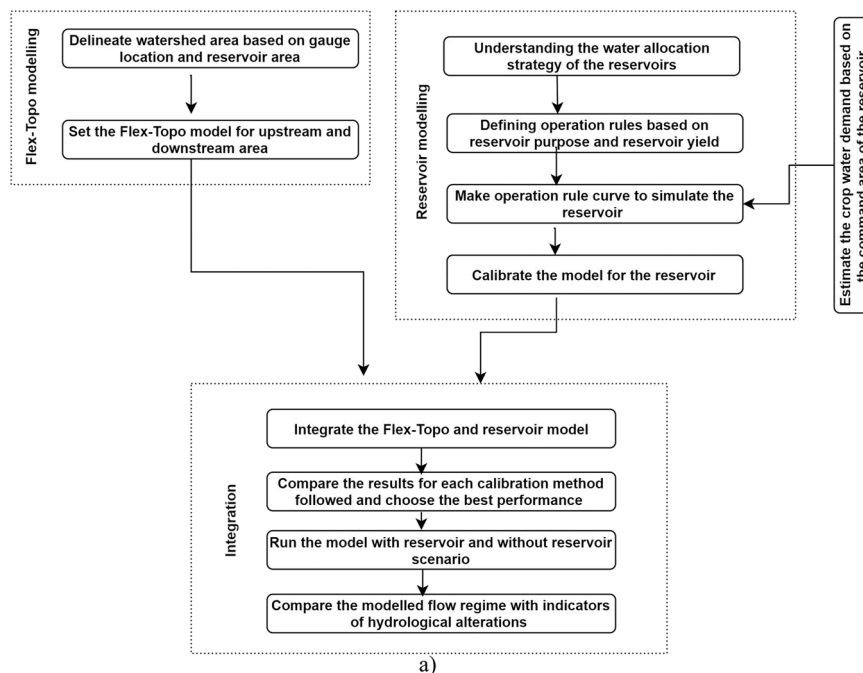


Fig. 2. The upper Cauvery basin. Reservoir sites selected for study are indicated in blue colour. Letters A B, C, and D refer to the command areas (shown in different colours) corresponding to the reservoirs, with the names of reservoirs and gauging stations indicated. The sub-basins corresponding to these gauging stations are also delineated and delineations are shown by grey lines.

**Table 1**  
Brief description of the reservoirs under study.

Reservoir	Year of construction	Sub-basin based on gauge location	Catchment area (10 <sup>6</sup> m <sup>2</sup> )	Gross Storage (10 <sup>6</sup> m <sup>3</sup> )	Depletion Period	Residence time (months)	Reservoir surface area to upstream area ratio	Filling period	Main purpose
Harangi	1982	Kudige	419.58	240.69	December-May	7.23	0.026	June - November	Irrigation
Hemavathi	1979	M.H. Halli	2810	1050.63	October-May	22.63	0.023	June - September	Irrigation + drinking water
Krishna Raja Sagara (KRS)	1938	Kollegal	10,619	1400.31	October-May	8.68	0.010	June - September	Irrigation + drinking water
Kabini	1974	T. Narasipur	2141.90	552.74	November - May	3.57	0.026	June - November	Hydropower + Irrigation



**Fig. 3.** (a) Overall methodology for analyzing the impact of reservoirs on flow regimes. (b) Modelling concept: Upstream and downstream contributing areas of the gauging station (GS) are modelled as F1 and F2 respectively. The top row shows how the reservoir model (RM) that contributes to irrigating a certain Command area is integrated with F1 and F2 and calibrated. In order to simulate the pre-dam situation, RM is removed from the calibrated model, along with its contribution to irrigate the Command area.

simulates the response of catchments based on different hydrological response units (HRUs). It approximates the river landscape hydrological behaviour by delineating catchments into different functional hydrological response units, e.g., wetland, hillslope, and plateau (Gharari et al., 2014). The novelty is that the model structure depends on landscape classes determined mainly by topography, which can include geological, geomorphological, or land-use classification (Savenije, 2010). The parsimonious model has proven to be transferable to data-scarce basins because its model structure is constrained by topography, relying less on data to calibrate parameters, and is robust in its simulations of flows under changing land-cover patterns (Gao et al., 2014; Savenije, 2010).

### 3.1.1. The Landscape classification

Topographic features like DEM, slope and Height Above the Nearest Drainage (HAND) are used to make the three broad classifications. The slope and HAND are processed in ArcGIS using DEM (80 m resolution). The overall watershed area was delineated based on gauge location. Again, the watershed area for F1 is delineated based on dam location. The F1 area is clipped from the whole watershed to get F2. For each F1 and F2, the raster data set including DEM, slope, HAND, and basin boundary are clipped and exported to Matlab for further analysis. Thresholds are selected to distinguish between the three landscape classes. Locations with HAND > 5 m and slope < 11 per cent is classified as a plateau, locations with HAND > 5 m and slope > 11 per cent is considered as hillslopes and locations with HAND < 5 m are considered wetlands (Gharari et al., 2011). The classified maps are then compared with land use maps and five HRUs (Hillslope forests, Hillslope crops, Plateau forests, Plateau crops, Wetlands) are determined based on the percentage of landscape classes for the upstream (F1) and downstream (F2) areas of the reservoir for each sub-basin.

### 3.1.2. The model structures

The FLEX-Topo model structure is graphically presented in Fig. 4, while the description of the variables of each hydrological response unit of the FLEX-Topo model is given in Table 2.

Rainfall  $P$  ( $\text{mm d}^{-1}$ ) is first partitioned between interception evaporation  $E_i$  ( $\text{mm d}^{-1}$ ) and effective rainfall  $P_e$  ( $\text{mm d}^{-1}$ ) based on a threshold  $S_{i, \max}$  (mm). Effective rainfall is partitioned between water retention in the soil and yield runoff  $R$  ( $\text{mm d}^{-1}$ ), based on the root zone storage capacity  $S_{u, \max}$  (mm) and a shape parameter  $\beta$  (-). Plant transpiration  $E_t$  ( $\text{mm d}^{-1}$ ) is calculated based on potential evaporation  $E_0$  ( $\text{mm d}^{-1}$ ), a soil moisture threshold parameter  $C_e$  (-) and the relative soil moisture  $S_u/S_{u, \max}$ . The generated runoff is further partitioned between a fast component  $R_f$  ( $\text{mm d}^{-1}$ ) and a slow component  $R_s$  ( $\text{mm d}^{-1}$ ) through a separator  $D$  (-). A lag function is applied to simulate the lag time  $T$  (d) between peak flow and storm event. Two linear reservoirs with different time constants  $K_f$  (d) and  $K_s$  (d) are used to calculate the fast and slow runoff. The total runoff  $Q_m$  ( $\text{mm d}^{-1}$ ) is the sum of the fast component  $Q_f$  ( $\text{mm d}^{-1}$ ) and the slow component  $Q_s$  ( $\text{mm d}^{-1}$ ).

The FLEX-Topo model classifies a landscape into different hydrological response units (HRUs) based on the elevation (DEM), slope and Height Above Nearest Drainage (HAND). The landscape is first divided into Hillslope, Plateau and Wetland and the classification is then compared with land use maps. More than 50 per cent of the area in the Cauvery basin is dominated by field crops followed by plantation crops and evergreen forests. The hillslope is characterized by comparatively larger root zone capacities due to deeper groundwater levels and perennial forest. But the land use pattern of the Cauvery basin has been heavily modified by agriculture. Five HRUs are then determined based on the percentage of landscape classes for the upstream and downstream areas of the reservoir for each sub-basin (Fig. 5). The main difference between these five HRUs is the structure of the unsaturated root zone reservoir ( $S_u$ ). Patterns of plant rooting depth bear a strong topographic and hydrologic signature at landscape scales (Fan et al., 2017). Therefore, The  $S_{u, \max}$  for hillslope forest and plateau forest have comparatively larger root zone capacities than hillslope crops and plateau crops. In the wetlands, the root zone storage capacity ( $S_{u, \max, W}$ ) is relatively low due to the shallow groundwater table. The five landscape units are connected to a common groundwater reservoir, recharged by hillslopes forest ( $R_{sl, HF}$ ), hillslopes crop ( $R_{sl, HC}$ ), plateau forest ( $P_{p, PF}$ ), plateau crop ( $P_{p, PC}$ ) and capillary rise ( $C_R$ ) from the wetlands. The model parameter ranges used during the calibration of the model are given in Table 3 and are set by optimization.

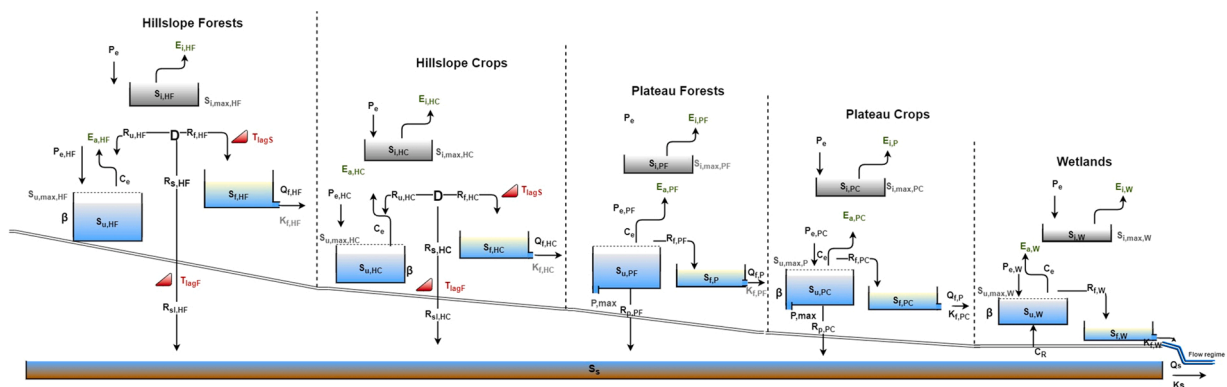


Fig. 4. The FLEX-Topo model structure used, showing that different landscape-land use classes have different model structures. All such structures additively contribute to the outflow.

**Table 2**

Brief description of the various variables linked to the FLEX-Topo model.

Variables	Description
P	Rainfall
P <sub>e, HF, P<sub>e, HC, P<sub>e, PF, P<sub>e, PC, P<sub>e, W</sub></sub></sub></sub></sub>	Effective rainfall
S <sub>i, HF, S<sub>i, HC, S<sub>i, PF, S<sub>i, PC, S<sub>i, W</sub></sub></sub></sub></sub>	Interception reservoir for hillslope forest, hillslope crop, plateau forest, plateau crop, and wetlands.
S <sub>u, HF, S<sub>u, HC, S<sub>u, PF, S<sub>u, PC, S<sub>u, W</sub></sub></sub></sub></sub>	Unsaturated reservoir for hillslope forest, hillslope crop, plateau forest, plateau crop, and wetlands.
S <sub>f, HF, S<sub>f, HC, S<sub>f, PF, S<sub>f, PC, S<sub>f, W</sub></sub></sub></sub></sub>	Fast reservoir for hillslope forest, hillslope crop, plateau forest, plateau crop, and wetlands
E <sub>i, HF, E<sub>i, HC, E<sub>i, PF, E<sub>i, PC, E<sub>i, W</sub></sub></sub></sub></sub>	An interception from hillslope forest, hillslope crop, plateau forest, plateau crop, and wetlands
E <sub>a, HF, E<sub>a, HC, E<sub>a, PF, E<sub>a, PC, E<sub>a, W</sub></sub></sub></sub></sub>	Transpiration from hillslope forest, hillslope crop, plateau forest, plateau crop, and wetlands
Q <sub>f, HF, Q<sub>f, HC, Q<sub>f, PF, Q<sub>f, PC, Q<sub>f, W</sub></sub></sub></sub></sub>	Runoff from fast reservoirs
S <sub>i, max</sub>	Storage capacity of the interception reservoir
C <sub>e</sub>	Fraction of S <sub>u, max</sub>
S <sub>u, max</sub>	Maximum capacity of the unsaturated zone (Equivalent to the soil moisture capacity in the root zone)
B	Spatial heterogeneity in the catchment
D	Splitter to separate recharge from the preferential flow
C, max	Capillary rise
K <sub>f</sub>	Recession coefficient between the fast and slow reservoir
P, max	Maximum percolation rate
R <sub>f, P</sub>	Sub-surface flow
R <sub>p, P</sub>	Recharge in groundwater

### 3.1.3. Reservoir inclusion in the FLEX-Topo model

Separate FLEX-Topo models are created for the contributing areas corresponding to the inflow points to the reservoirs and river reaches between the reservoir outflow points and downstream flow gauging stations. Fig. 5 illustrates it in greater detail, where for each reservoir case upstream area F1 and downstream area F2 are modelled separately. A separate reservoir operation model is created for each reservoir. Thus, for each basin with a reservoir, FLEX-Topo for F1 models the inflow to the reservoir. The operation model of the reservoir then determines inflow to the area F2, and the FLEX-Topo model for this area then determines the outflow at the downstream gauge station. The outflows from Kudige, M.H. Halli and T. Narasipur sub-basins are treated as inflows to the Kollegal sub-basin at their respective gauging stations (See Fig. 5). An attenuation factor ranging between 0 and 1 is considered to account for any water loss from the outflow of the reservoir to the gauge station for which the outflow is being modelled.

### 3.1.4. Reservoir operation and modelling

Reservoir operation is modelled using a shortage rule curve based on water demand for each reservoir. Depending on the end-user demand that a reservoir is catering to, the following conservation of mass equation is modelled for each time step:

$$\frac{S_{t+1} - S_t}{\Delta t} = I_t + O_t - E_t + P_t - (L_t * D_t) \quad (1)$$

Where, S=storage, I<sub>t</sub> =inflow, O<sub>t</sub> =outflow, E<sub>t</sub> =evaporation from reservoir surface, P<sub>t</sub> =precipitation on reservoir surface, D<sub>t</sub> =demand for reservoir water, L<sub>t</sub> = fraction supply of the demand for the reservoir on day t and Δt = 1 day.

### 3.1.5. Operation rule curves

The reservoir operations are based on shortage rule curves which define zones within which specified proportions of the demand are supplied (Basson et al., 1994). These supply zones in turn depend on reservoir functions, which include flood control, irrigation, hydropower, and water supply. Three operating rule curves for 100 per cent demand-supply (L=1.0), 80 per cent demand-supply (L=0.8), and 50 per cent demand-supply (L=0.5) are used to obtain four operating zones, i.e., spill zone, flood control zone, conservation zone and buffer zone (See supplementary materials Figure S.1). The operating rule curve is defined based on trigonometric functions developed by Ndiritu and Sinha (2009) as indicated below:

$$L_t = \tau + (3 - 1)w + a \left( \sin \left( 2\pi \left( \frac{t}{365} - \ell \right) \right) \right) \quad (2)$$

Where, L<sub>t</sub> is the operation rule curve for a different fraction of demand-supply level for the t<sup>th</sup> time step (t = 1, 2, 3, ..., 365 days),

τ = Translational Parameter.

w =Width parameter.

a =Amplitude parameter.

ℓ = Lag parameter.

The four supply zones derived from three operating rule curves serve as the metric to determine the extent to which demands are met all year round. The demand is then calculated on a daily time step and depending on the purpose of the reservoir with respect to the three operating rule curves. Table S.2 (see supplementary materials) shows the range of the various parameters of the operating rule curve equation that are used to calibrate the reservoir operation rules such that the assumptions stated in Table S.1 (see supplementary materials) are obeyed. Based on the purpose of the reservoir (irrigation or hydropower) as defined in the shortage rule curve, different levels of demand are satisfied. Fulfilling the different levels of demand is subjected to multiple reliability constraints of demand and



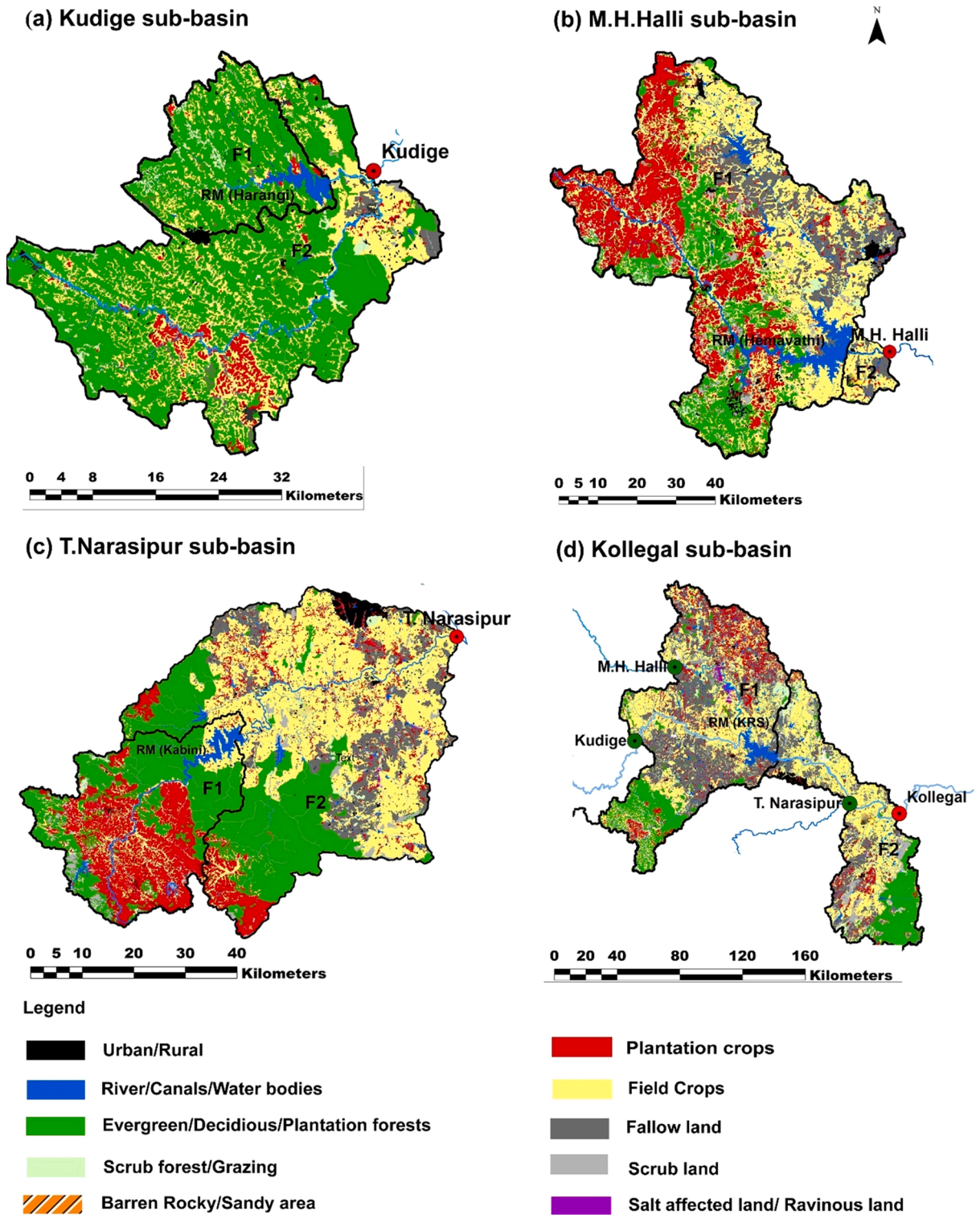


Fig. 5. Landcover map shown for each basin. Also shown are the reservoirs, and the corresponding upstream and downstream areas. The three entities are connected to model the stream flows at the reported gauge stations indicated in the red dot. The outflows from Kudige, M.H. Halli and T. Narasipur sub-basins are added to the Kollegal sub-basin at the gauging stations indicated by the green dots (shown in Figure d).

**Table 3**

Model parameters prior ranges. These define the feasible range within which parameters are calibrated.

Parameters	Parameter Range				
	Plateau crop	Plateau forest	Hillslope crop	Hillslope forest	Wetlands
$I_{max}$ [mm/day] (Storage capacity of the Interception reservoir)	1–8	6–10	1–8	6–10	1–5
$C_e$ [-] (Fraction of $S_{u, max}$ )	0.1–1	0.1–1	0.1–1	0.1–1	0.1–1
$S_{u, max}$ [mm] (Maximum soil moisture capacity in the root zone)	100–500	100–1000	100–500	100–1000	10–100
$\beta$ [-] (Spatial heterogeneity in the catchment/shape parameter)	0.1–5	0.1–5	0.1–5	0.1–5	0.1–5
$P_{max}$ [-] (Maximum percolation rate)	0.1–5	0.1–5	–	–	–
$D$ [-] (The splitter)	–	–	0–0.5	0–0.5	–
$C_{Rmax}$ [mm/day] (Capillary rise)	–	–	–	–	0.01–1
$K_f$ [d] (Recession coefficient of the fast reservoir)	0.005 – 1	0.005 – 1	0.005–1	0.005–1	0.005–1
<b>Catchment parameters</b>					
$K_s$ [d] (Recession coefficient of the slow reservoir)	0.0001–0.01				
$T_{lag}$ [d] (Time lag between the storm and peak flow)	0.1 – 30				
Frac 1 [-] (Fraction of forests cover)	The value is fixed (0 –1) based on the percentage of forest area in the sub-basin				
Frac 2 [-] (Fraction of Irrigation)	The value is fixed (0 –1) based on the percentage of Irrigated area in the sub-basin				

Source: Gharari et al. (2014); Gao et al. (2016)

reservoir storage state and optimization is carried out using the Non-Dominated Sorting Genetic Algorithm (NSGA-II) optimization method. The reservoirs in the Kudige sub-basin serve the sole purpose of meeting the irrigation demands. The Hemavathi and Krishna Raja Sagara in M.H. Halli and Kollegal sub-basins are used for irrigation and drinking purpose. The Kabini reservoir in the T. Narasipur sub-basin is used for both irrigation and hydropower production. The area capacity curve for the Kabini reservoirs is estimated to maintain the water level around the reference level using the least square fitting method. For details, see [supplementary materials](#)

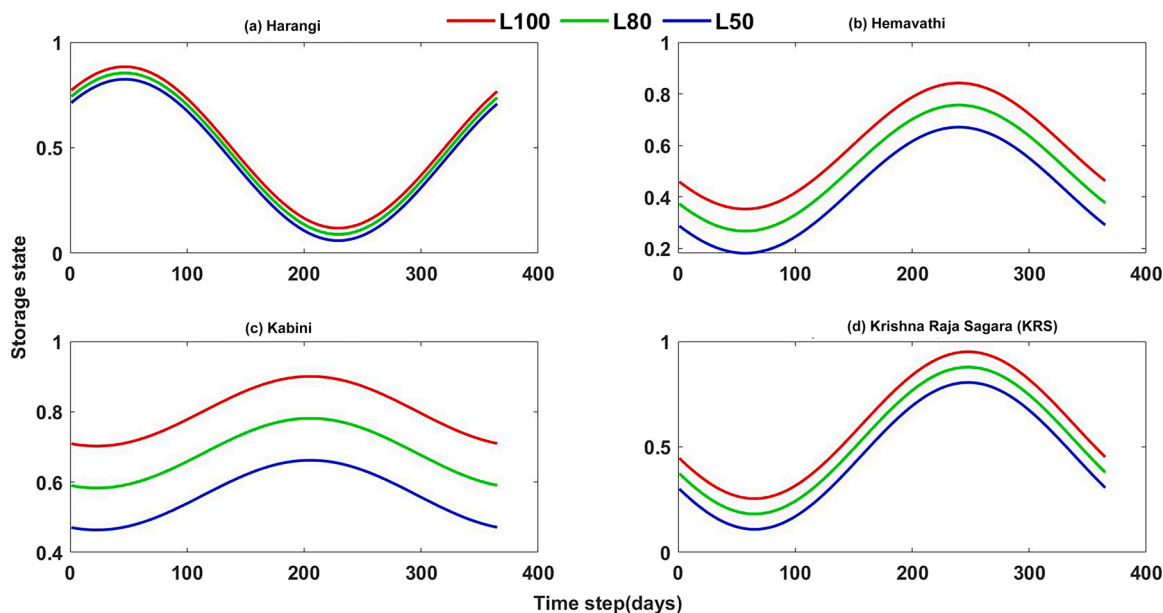


**Fig. 6.** The calibrated shortage rule curve of reservoirs under study. The x-axis shows the days of a year whereas the y-axis shows the fraction of total available storage (dimensionless storage state).

section 1.1.

The shortage rule curves of different reservoirs studied are shown in Fig. 6. The L50, L80 and L100 refer to 50 per cent, 80 per cent and 100 per cent supply of demand. For Hemavathi, Harangi and KRS reservoirs, the storage state of the reservoir can decrease below 20 per cent to fulfil the irrigation demands but cannot go below the L50 curve as this is the critical limit that determines whether to cut back the water for irrigation or any kind of public use. To maintain the function of flood control, the upper limit curve will not be changed for all the reservoirs. In the case of the Kabini reservoir, which is used for hydropower production, the lower limit defines the hydropower generation and therefore the lower limit (L50) will always be more than 40 per cent of the storage state. More details about reservoir modelling are given in the [supplementary materials](#).

### 3.2. Data input to the model

Rainfall and potential evapotranspiration are used as forcing data. Daily gridded rainfall ( $0.25^\circ \times 0.25^\circ$ ) and temperature ( $1^\circ \times 1^\circ$ ) data are obtained from the Indian Meteorological Department, Government of India (Pai et al., 2014; Srivastava et al., 2009). The rainfall and temperature information is extracted for each sub-basin to force the FLEX-Topo model and the reservoir model. The potential evapotranspiration ( $ET_p$ ) is calculated based on the Hargreaves equation (Hargreaves and Samani, 1982) considering max, mean and min temperature values.

The runoff data are acquired from the Central Water Commission, Government of India (CWC, 2018). The data on reservoirs including inflow, outflow and storage level is accessed from Karnataka State Natural Disaster Monitoring Centre, Government of Karnataka, India. ([https://www.ksndmc.org/Reservoir\\_Details.aspx](https://www.ksndmc.org/Reservoir_Details.aspx)). The crop water demand is calculated using crop-coefficient (for more details, see [supplementary materials](#), Section 2).

### 3.3. Model calibration

The dataset from January 1991 to December 2010 is used to calibrate the FLEX -Topo models and the data set from 2010 to 2016 is used for validation. The reservoir models are calibrated using the dataset from January 2011 to December 2016 to obtain the reservoir operating rules first. The calibration of a FLEX-Topo model integrated with the reservoir of each basin is conducted in a stepwise manner.

Four calibration strategies are considered for each reservoir location as indicated in Fig. 7(a, b). First (called “R and F”) the integrated FLEX-reservoir model is calibrated using the downstream gauging station. In this calibration strategy, the model generated for each reservoir in each sub-basin is first integrated into the corresponding upstream and downstream FLEX-Topo models of the sub-basin. Then the output of the system of models, i.e., the F-R-F model, is calibrated using Monte-Carlo sampling on observed streamflow at the corresponding gauging station.

In the second calibration method (called “R then F”) the reservoir is calibrated first, then keeping the parameters of the reservoir fixed the integrated model is calibrated using a downstream gauging station. The parameters of the reservoir model are calibrated first using the reservoir’s inflow and outflow data from January 2011 to December 2016. The reservoir parameters are then fixed to the best parameter set and calibrated reservoir model is inserted in the serial system of models F-R-F, The FLEX-Topo model parameters are then calibrated using data from the downstream gauging station for each sub-basin.

Third (“R and F separately”), both the reservoir model and FLEX-Topo model are calibrated separately. Parameters of the Flex-Topo are transferable (Gao et al., 2014). Therefore, the reservoir and the Flex-Topo model of the entire sub-basin are calibrated separately

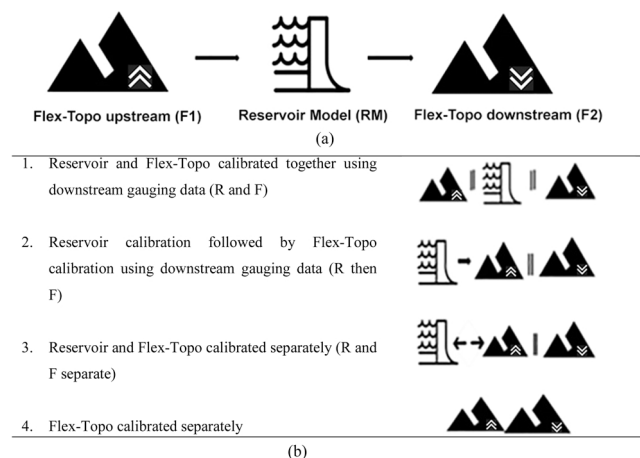


**Fig. 7.** (a): The F-R-F model conceptualization is composed of a FLEX-Topo model for the contributing area upstream of a reservoir (F1), a reservoir model (RM) and a FLEX-Topo model for the contributing area downstream of the reservoir (F2) Fig. 7(b): Different strategies to calibrate the integrated the F-R-F model.

and then the calibrated parameters are used to run the system of the models (i.e., the F-R-F model).

In the fourth method, the FLEX-Topo model for each sub-basin is calibrated and assessed separately to compare the results with the above three calibration methods. All the parameters are considered independent of each other. Modelled runoff corresponding to each parameter set is compared with the observed using Nash-Sutcliffe Model Efficiency (NSE) and Mean Absolute Error (MAE). The results indicated that the second calibration method (R then F strategy) performed well during the calibration and validation phase compared to the other methods, therefore, the reservoir calibration followed by the FLEX-Topo calibration method is adopted for final calibration.

The spatial heterogeneity, as well as variations in land use, has been incorporated in F1 and F2 which define the model structures and fluxes of FLEX-Topo (as shown in Fig. 5). Slope, height above the nearest drainage and land use type together defines the various model classes (or landscapes) and associated with each such 'type' of the landscape is a model structure with its unique equations (see Fig. 4). For example, within F1 forested hillslopes have a model structure that replicates subsurface flow processes while areas that are close to river networks such as wetlands have model structures that simulate processes such as saturation excess overland flow. Further, evaporation fluxes from forested hillslopes are modelled differently from the evaporation from forested agriculture areas. Since the parameters of FLEX-Topo are transferable (Gao et al., 2014), the same parameters have been used, and calibrated jointly, from similar heterogeneities such as for forested hillslopes in F1 and F2. Given that topography controls the model structures, the FLEX-Topo model is calibrated based on streamflow observed at the corresponding stations downstream of the reservoirs.

The Elitist Non-Dominated Sorting Genetic (NSGA-II) algorithm is used to calibrate the model parameters (Deb et al., 2000). NSGA-II is a multi-objective optimization algorithm. It simultaneously optimizes multiple objectives by identifying parameters that yield model performances that are not dominated by any other feasible parameters in the multi-objective space (Efstratiadis and Koutsoyiannis, 2010).

Two objective functions are defined and minimized simultaneously. The first objective ( $f_1$ ) is the negative of Nash-Sutcliffe Efficiency (NSE) and the second objective ( $f_2$ ) is the Mean Absolute Error (MAE).

$$f_1 = -NSE = -1 + \frac{\sum_{i=1}^n (Q_i^o - Q_i^m)^2}{\sum_{i=1}^n (Q_i^o - \bar{Q}_o)^2} \quad (3)$$

$$f_2 = MAE = \frac{1}{n} \sum_{i=1}^n |Q_i^o - Q_i^m| \quad (4)$$

Here,  $Q_i^o$  is the  $i^{th}$  observation for the observed discharge.  $Q_i^m$  is the  $i^{th}$  value of the modelled discharge being evaluated.  $\bar{Q}_o$  is the mean of observed discharge and  $n$  is the total number of observations. The parameter sets calibrated for the FLEX-Topo model and the reservoir model are given in Tables 3 and 4 respectively.

The NSGA-II parameter setting may have different impacts on computational effectiveness. The population crossing over and population mutation plays critical roles during optimization (Wang et al., 2019). Usually, the higher fraction of the population crossing over (0.9) and a lower value of mutation value is preferred for better convergence and to prevent the population from getting trapped in local optima (Wang et al., 2019). The population size depends on the number of the decision variables calibrated in the model and keeping the population size five times the number of decision variables is considered ideal for the simulation (Gutierrez et al., 2019). Since for FLEX-Topo, there are 20 parameters, the population size is kept at 100. Similarly, for the reservoir model, the number of parameters is five, which translates into a population size of 25. Higher population sizes were also attempted but not used and reported for later analysis because the performance achieved was similar to the reported population sizes. The number of iterations is first tested using 50, 100, 250 and 500 iteration runs and 250 was finally chosen based on the best optimization results.

For each parameter set, the modelled run-off at stations shown in Fig. 5 is compared with the observed runoff using -NSE and MAE (equations 3 and 4). The Pareto-front corresponding to the minimum value of -NSE and MAE as identified by the NSGA-II algorithm is considered as containing the better performing parameter sets for each of the four basins.

### 3.4. Indicators of hydrological alterations

The set of Indicators of Hydrological Alteration (IHA) initially proposed by Richter et al. (1996) is used to understand the impacts of

**Table 4**  
Parameter setting for NSGA II optimization of the model.

NSGA parameters	Reservoir calibration	Integrated FLEX-Topo calibration
No. of Iterations	250	300
No. of decision variables	5–8	25
No. of population size	25–40	125
Population Crossover	0.7	0.7
Population Mutation	0.2	0.2
New generation selection	Elitist selection	Elitist selection
Ordering criteria	Crowding distance	Crowding distance

reservoirs on the flow regimes in the Cauvery basin. The parameters considered in IHA have a strong relationship with the river ecosystem and the degree of human interferences in the form of dams, barrages, and other kinds of water diversions on flow regime can be easily estimated. The IHA are categorized into five groups in terms of the magnitude of monthly flow, magnitude and duration of annual extreme flow condition, frequency, and duration of high and low flows (see [supplementary materials](#), Table S.5). In the present case study, the observed frequency corresponds to the modified flow regime due to reservoir construction and the expected frequency refers to the predicted flow regime without the reservoir.

## 4. Results

### 4.1. Reservoir calibration

The reservoirs are calibrated on a daily time scale. Due to limited data on reservoirs, all the years were used for calibration. There is no validation performed for the modelled streamflow at the reservoir outlets. The results of the reservoir calibrations are presented in [Table 5](#). Within parentheses, the Pareto front ranges produced by the NSGA II algorithm are given for both -NSE and MAE. The MAE is always non-negative, and a lower value means a better prediction. The MAE value of all four reservoirs falls in the range of 0.71–2.92 ( $10^6 \text{ m}^3 \text{ day}^{-1}$ ) which is in the acceptable range. Similarly, the NSE value was observed between 0.51 and 0.73. The NSE value above 0.50 is acceptable. [Fig. 8](#) compares the modelled outflows with the observed ones for the four reservoirs. It was observed that Krishna Raj Sagara (KRS) reservoir, which is the biggest reservoir among the studied sample, has fluctuating outflows during the low flow periods. The adopted operational rule curve within the reservoir models only considers water demands for irrigation or hydropower and does not model water releases for specific purposes, such as drinking water from the KRS dam. This is especially so during the low flow period that is thus not well captured by the model.

### 4.2. Integration of reservoirs with FLEX-Topo: F-R-F model calibration and validation

The calibration metrics of the models after the integration of corresponding reservoirs with the FLEX-Topo models are presented in [Table 5](#) and how the modelled streamflow time series compare with the observed are shown in [Fig. 9](#). The figure also shows the modelled stream flows that simulate the pre-reservoir cases (“No-Res”) for the four sub-basins. Here for each reservoir model that is integrated, a parameter set corresponding to a point that lies in the middle of the Pareto front in the objective space, i.e., balanced by non-dominated sets on either side, is chosen.

The scatter plots of the observed and modelled stream flows are shown in [Fig. 10](#). Amongst the four sub-basins, Kudige performed the best in calibration ( $R^2 = 0.90$ ) and validation ( $R^2 = 0.81$ ). Harangi is in the Kudige sub-basin, which is the smallest reservoir among all the reservoirs taken for the study. As indicated in [Table 1](#), the residence time of the Harangi reservoir is small, which meant that the reservoir model (being a more difficult calibration problem) had little impact on the overall model performance. The R-squared of M.H. Halli, T. Narasipur and Kollegal performed in the range of 0.73–0.77 during the calibration phase and 0.67–0.74 during the validation phase. The models of all the basins, therefore, appear to have a bias in predicting flows, with modelled daily flows being higher than the observed-on average for T. Narasipur and Kollegal sub-basins.

[Table 5](#) reports on the performance of the calibrated F-R-F model with the observed for the four sub-basins. The NSE was observed

**Table 5**

The model performance metrics for the calibration of the four reservoirs and the calibration and validation of the F-R-F models (i.e., the integration of calibrated reservoirs with upstream and downstream FLEX-Topo models) for the corresponding four sub-basins.

Reservoir calibration (2011–2016)						
Reservoirs	-NSE [range]			MAE [range] ( $10^6 \text{ m}^3 \text{ day}^{-1}$ )		
Harangi(kudige)	-0.64 [- 0.65 - (-0.63)]			2.92 [ 2.92 - 3.01]		
Hemavathi(M.H. Halli)	-0.51 [- 0.52 - (-0.51)]			1.15 [1.15 - 1.16]		
Kabini (T. Narasipur)	-0.73 [- 0.73 - (-0.72)]			1.24 [ 1.24-1.24]		
KRS(Kollegal)	-0.68 [- 0.67 - (-0.69)]			0.71 [0.70-0.72]		
F-R-F model calibration and validation						
Sub-basins	Calibration (1991–2010)			Validation (2011–2016)		
	-NSE [range]	MAE [range] ( $\text{mm day}^{-1}$ )	PBIAS (%)	-NSE	MAE ( $\text{mm day}^{-1}$ )	PBIAS (%)
Kudige	-0.80 [- 0.81 - (-0.80)]	1.36 [1.33 - 1.39]	8.54	-0.65	2.05	16.27
M.H. Halli	-0.57 [- 0.57 - (-0.56)]	0.37 [0.40 - 0.41]	3.24	-0.52	0.48	17.66
T.Narasipur	-0.53 [- 0.53 - (-0.50)]	0.67 [0.67-0.69]	11.62	-0.52	0.66	-42.80
Kollegal	-0.53 [- 0.54 - (-0.52)]	0.92 [0.92 - 0.97]	-6.23	-0.50	0.86	-57.54

**Note** - The value indicates the best-performing parameters following the minimum Euclidean distance. The figures in parenthesis indicate the pareto-optimal range of all solutions considered feasible.  $\text{PBIAS} = 100 \frac{\sum_{i=1}^n (Q_i^o - Q_i^m)}{\sum_{i=1}^n Q_i^o}$  is provided only for the F-R-F model to evaluate its performance for the four sub-basins.

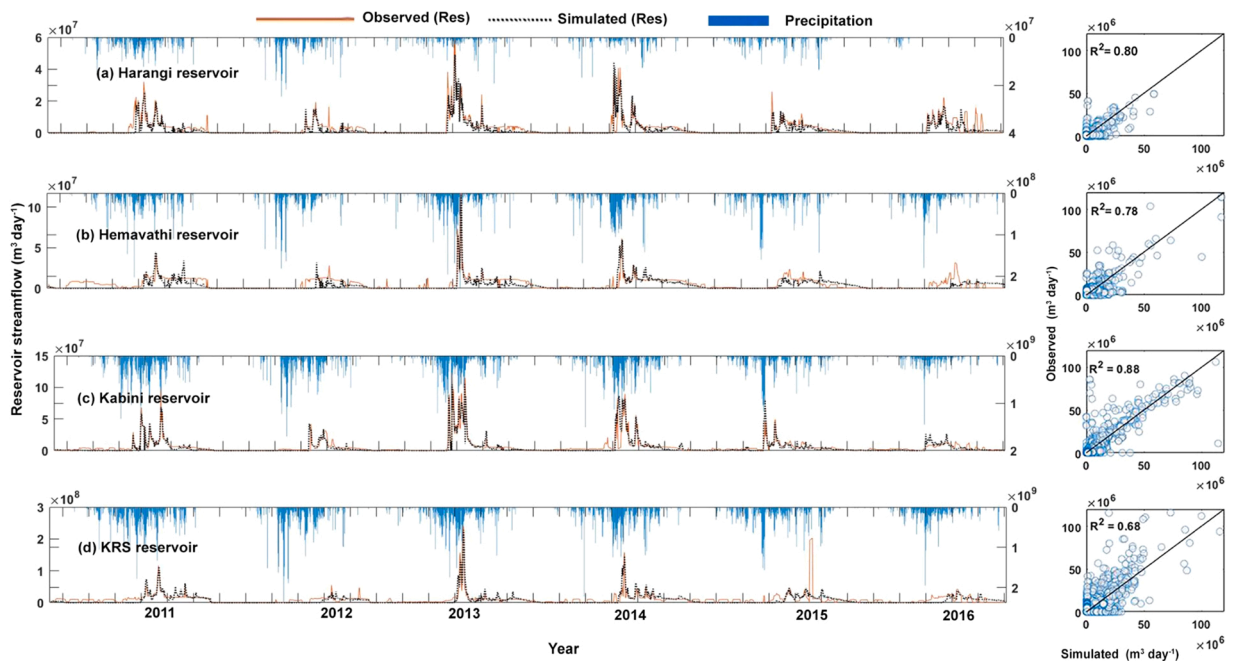


Fig. 8. The calibration performance of the reservoir models for the four reservoirs (reservoir outflow in  $\text{m}^3 \text{day}^{-1}$ ).

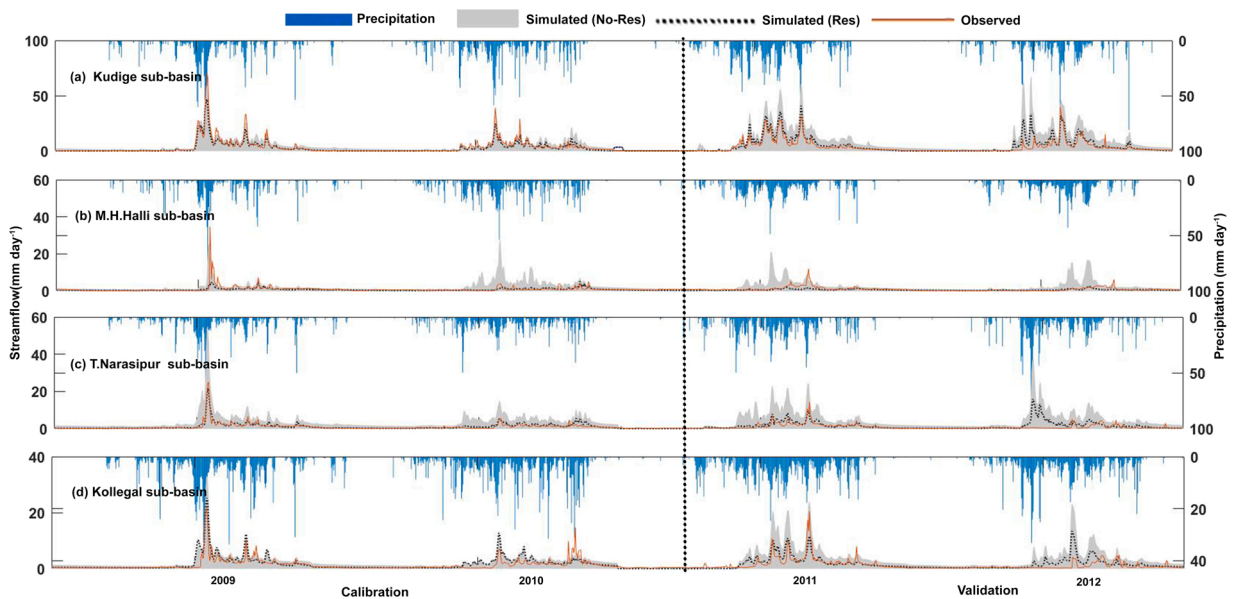
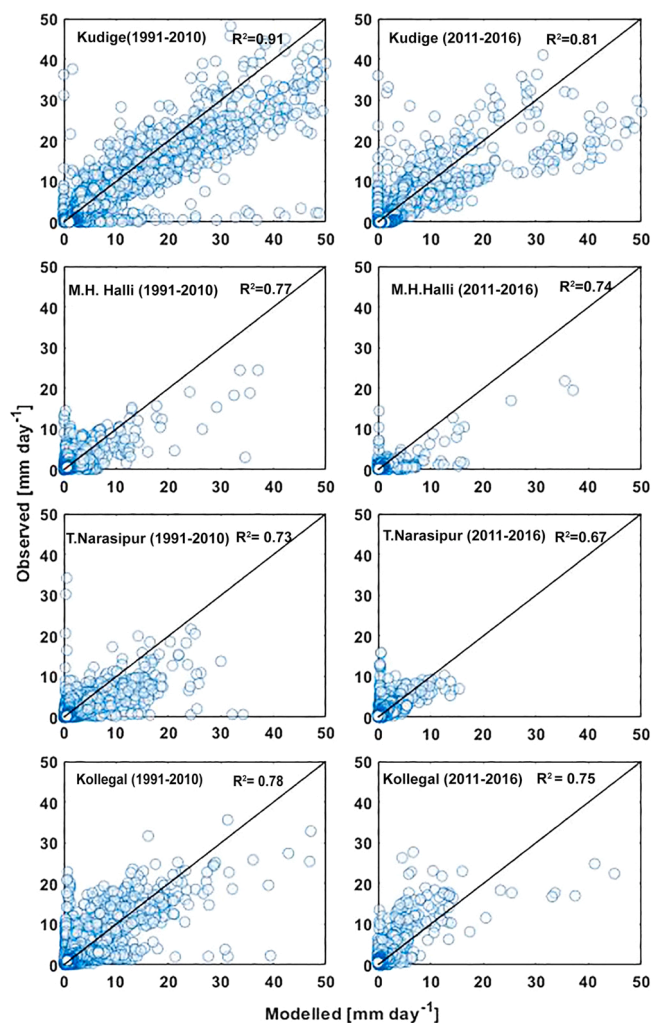


Fig. 9. The F-R-F model performance for the four sub-basins. Only four years (2009–2012) are presented here and the plots for the entire calibration and validation periods are given in S.5 in the [supplementary materials](#). Additionally, ‘No-Res’ represent simulations without reservoirs and ‘Res’ represent simulations with reservoirs.

in the range of 0.53–0.80 in the calibration phase and 0.50–0.65 in the validation phase for all four sub-basins. The NSE value above 0.50 is considered an acceptable level of performance. Similarly, the values of MAE were observed in the range of 0.92–1.36 mm/day in the calibration phase and 0.86–2.05 mm/day in the validation phase and are acceptable. The PBIAS values for the calibration and validation periods are also provided in Table 5. It indicated that for Kudige and M.H. Halli, the values of PBIAS are within the  $\pm 25$  per cent limits, which are acceptable. However, for T. Narasipur and Kollegal sub-basins the PBIAS values of the validation periods are beyond the acceptable limits.

The mostly positive PBIAS values suggest that the low flows are better simulated than the high flows. This is also evident in Fig. 8 where high flows are often missed, especially in the cases of Harangi, Hemavathi and Kabini reservoirs. Since the parameter sets on the



**Fig. 10.** Scatter plot of the observed and modelled stream flows during calibration (left panel) and validation phase (right panel) for the four sub-basins.

pareto front that are closest to the origin are chosen for the simulations, the corresponding model simulations do not have the best possible performances in either of the two objective functions. Even though NSE is used as one of the objective functions (that is sensitive to high flows due to NSE being a quadratic function of the residuals), MAE is the other objective function that is robust to outliers (Pande, 2013b; Pande, 2013a). This may be a reason why high flows are not as well simulated as low flows.

#### 4.3. Impacts of the reservoirs on the flow regimes

The impacts of the reservoirs on the river flow regimes are assessed using indicators of hydrological alteration (Richter et al., 1996). The calibrations of the entire basins at the gauge sites are not possible to estimate the pre-reservoir scenarios due to the lack of data before the dams were constructed. Furthermore, the calibration of the upstream models (F1) using inflow data of the reservoirs was hampered by limited data on the reservoirs themselves, which were available for six years within the period studied. Therefore, the calibrated F-R-F models are used to infer the natural flow regimes by removing the reservoirs of the corresponding four sub-basins. The flow regimes simulated by the models after removing the reservoirs are used as pre-impact simulations for the corresponding sub-basins. The gauge stations, used for model calibration and validation, located downstream of the reservoirs are used to compare the pre-and post-construction of reservoirs (see Fig. 5 for gauge station locations) and the data from the year 2001–2016 is used for calculating the indicators for hydrological alterations.

##### 4.3.1. Impact on the magnitudes of the monthly stream-flow conditions

The median values of the monthly stream flow for the four sub-basins are given in Fig. 11. It shows that the flows in the sub-basins were consistently reduced during all the months of the year after the reservoirs were constructed.

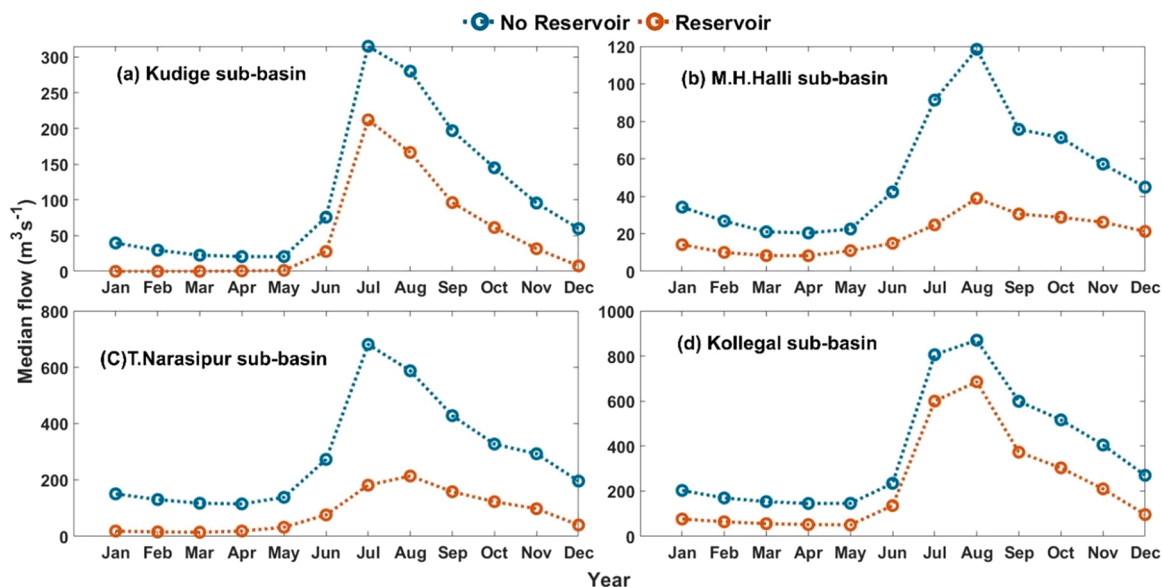


Fig. 11. The magnitudes of the monthly streamflow pre- and post-reservoir construction.

#### 4.3.2. Impact on minimum flows

The median values of hydrological alterations for the annual extreme flow conditions of the upper Cauvery river basin are given in Table 6. The 1-day and 3-day minimum median flows were reduced significantly in all sub-basins. Zero flow days were observed only in the Kudige sub-basin in the post-impact period. The base-flow indices of all basins were reduced after reservoir constructions, except for the M.H.Halli sub-basin, where the base-flow index increased.

#### 4.3.3. Impact on the maximum flows

The median values of the impact of reservoirs on maximum flows are also indicated in Table 6. All 1-day and 3-day maximum median flows were reduced in all sub-basins, and most significantly in the M.H.Halli and T.Narasipur sub-basins, where high-magnitude flooding was eliminated after reservoir constructions.

#### 4.3.4. Impact on the frequency and duration of high and low pulses

The high and low flow conditions are defined based on 75th (high pulse) and 25th flow (low pulse) percentiles. Increases in the low pulse durations are observed in the Kudige, M.H.Halli and Kollegal sub-basin which may worsen the eco-hydrological environment of the river and surrounding floodplains. A decrease in low pulse duration is observed in the T.Narasipur sub-basin. Moderate decreases in high pulse durations are observed in all the sub-basins. A decrease in high pulse duration hampers the supply of nutrients to the aquatic plants and animals and may reduce the riverine biodiversity. This means that the supply of nutrients may have been hampered in all the sub-basins affecting riverine biodiversity.

In the context of a hydropower reservoir (Kabini), it was observed that the reservoir case has long low pulse duration than the case without a reservoir. Since a specific water level should be maintained in the hydro-power reservoir to generate electricity, water is frequently discharged from the reservoir to do so resulting in low pulse duration. In contrast to the hydropower reservoir, irrigation reservoirs (Harangi, Hemavathi and KRS) have higher low pulse durations than for its corresponding no reservoir cases. This suggests that, in comparison to hydropower reservoirs, irrigation reservoirs generate higher flow regimes. A similar reduction in low pulse duration was observed in the Yangtze River due to reservoir operation for irrigation purposes in China (Gao and Wang, 2018).

## 5. Discussion

The method implemented in this paper is limited by various assumptions. After discussing the assumptions and how these may be alleviated, the influence of reservoir operations on flow regimes in the upper Cauvery are synthesized and followed by what it may imply for reservoir operations in India.

### 5.1. Model uncertainty and underlying assumptions

The result indicates that flow regimes are clearly altered from their natural state following reservoir impoundments. Although dams differ dramatically in size, function, and location, almost all sub-basin record a reduction in median flow, minimum and maximum flows. These patterns are primarily caused by regulated reservoir operations, including storing and releasing flows for irrigation, or hydropower generation, which alters the river streamflow characteristics. Moreover, the water is being diverted for irrigation outside



**Table 6**  
Indicators of hydrological alterations of extreme flow conditions.

IHA parameter	Kudige (Harangi) Irrigation		M.H.Halli (Hemavathi) Irrigation		T. Narasipur (Kabini) Hydropower		Kollegal (KRS) Irrigation	
	No Reservoir	Reservoir	No Reservoir	Reservoir	No Reservoir	Reservoir	No Reservoirs	Reservoirs
	Extreme flow condition ( $\text{m}^3\text{s}^{-1}$ )							
1-day minimum	15.43	0.00	17.55	7.11	97.22	12.45	127.4	44.98
3-day minimum	15.65	0.00	17.72	7.15	97.76	12.53	128.2	45.14
1-day maximum	1120.00	809.10	750.20	169.30	2450.00	877.20	3646	3027
3-day maximum	1041.00	713.90	680.9	138.5	2280.00	809.50	3474	2873
Number of zero days	0.00	90.50	0.00	0.00	0.00	0.00	0.00	0.00
Base flow index	0.14	0.00	0.26	0.30	0.30	0.12	0.28	0.16
	Frequency and duration of high and low flows ( $\text{m}^3\text{s}^{-1}$ )							
Low pulse count	4.00	2.50	4.00	4.00	2.00	5.5	2.00	2.00
Low pulse duration	9.00	52.75	13.50	19.50	25.50	7.75	18.5	117.5
High pulse count	5.00	6.00	4.50	3.00	5.50	3.00	6.00	5.50
High pulse duration	8.00	4.50	7.00	4.00	9.00	4.00	8.00	5.00

the basin which also contributed to altered flow regime characteristics. However, the diverted flow is not addressed in the present simulation in the sense that we assume that the irrigation water supply evaporates and does not return to the basin. This implies that the model is likely under-estimating available discharges at the sub-basin outlets and this has been reflected in the PBIAS values of T. Narasipur and Kollegal sub-basins during the validation phase.

In case of no reservoir, the command areas irrigated by reservoirs become unirrigated and the irrigated areas are reduced proportionally in the model based on the command area falling in the upstream and downstream areas of the reservoirs. Such an assumption needs to be validated, e.g., based on official records on land use types in the pre-reservoir periods.

The low flows are better simulated than the peaks. One explanation may be that the parameter sets on the pareto front that are closest to the origin are chosen for the simulations. This means that the corresponding model simulations do not have the best possible performances in either of the two objective functions. Even though NSE is used as one of the objective functions (that is sensitive to high flows due to NSE being a quadratic function of the residuals), MAE is the other objective function that is robust to outliers (Pande, 2013b; Pande, 2013a). This may be a reason why high flows are not as well simulated as low flows. The use of additional objective functions such as log (NSE) and others based on hydrological signatures (Santos et al., 2018) may alleviate such concerns.

The reservoirs were calibrated first partly because of limited data (following R then F calibration strategy). Only six years of daily scale time series were available for the inflows and outflows of the reservoirs, which was not deemed sufficient for the calibration and validation of the F-R-F model. Therefore, different time series are used for the calibration of FLEX-Topo and reservoir models. Further, because a standard operating rule curve is used for all the reservoirs, it is acknowledged that some of the dams' specific water discharges may not have been captured by the reservoir model. Validation results also suggest that modelled flows of two reservoirs are biased. Model calibration may therefore benefit from operating rule curves inspired by specific reservoir functions and flow requirements.

## 5.2. Influence of reservoir operations on flow regimes in the upper Cauvery

The study confirms that the average monthly flow in the Upper Cauvery basin is greatly influenced by reservoir operations and subsequent water abstractions in the basin. The reduction of streamflow in most of the months is likely contributing to the increased scarcity of water in different seasons. The decrease in monthly flows is observed across all the sub-basins throughout the year due to reservoir operations when compared to its natural flow regimes. The different operation rules in different sub-basins have varying degrees of influence on downstream flow timing, pulse behaviour, change rate, and frequencies of flow (Wang et al., 2016).

The decrease in summer flows during the post-reservoir periods, as evident from the model results, may lead to negative effects on the aquatic habitats and migratory and reproductive biology of fish species in the downstream areas. The one-day minimum flow at Kudige was observed to be below  $1 \text{ m}^3\text{s}^{-1}$ , which before the reservoir construction was  $15.43 \text{ m}^3\text{s}^{-1}$  and at a safe level. This huge reduction is harmful to the survival of aquatic organisms. The frequency and duration of high and low pulses are critical to supporting the migratory behaviour of fish during the spawning season (Wang et al., 2016). This has also been validated by some studies that have indicated that after the construction of reservoirs, the reduction in flows and changes in natural flow pulses threatened the survival of migratory fish species *Tor pituitora* in the Cauvery basin (Pinder et al., 2015). In addition, variations in fish assemblage structures have likely been affected since the structures are strongly associated with mean daily flows, base flow, number of zero-flow days and high-flow pulses (Arthington et al., 2014; Anderson et al., 2006; Perkin and Bonner, 2011). Furthermore, in the Kudige sub-basin, a period of 90 days of zero flow was recorded after the construction of the Harangi reservoir which created a stressful environment for the aquatic organisms.

In the T.Narasipur sub-basin, the natural base flow index of 0.30 was reduced to 0.12 after the construction of the Kabini reservoir. In tropical rivers, the streamflow discharge is composed entirely of the base flow through most of the dry season of the year (Smakhtin, 2001). This extended duration of zero flow leads to the loss of lotic habitats which places aquatic species at high risk of extinction (Mallen-Cooper and Zampatti, 2020).

The frequency and duration of low pulses were also impacted across all the studied sub-basins. Decreases in low pulse durations in the Kudige, M.H. Halli and Kollegal sub-basins may worsen the eco-hydrological environment of the river and surrounding floodplains. In contrast, an increase in low pulse duration was observed in the T. Narasipur sub-basin where the hydro-power reservoir is located. The reservoir releases excess water to preserve flood control capacity from June till August, after which it releases flow to meet the power generation requirements, which then increases the low flow duration in the T. Narasipur sub-basin.

Hydrological connectivity between the river channels and floodplain is dependent on the intensities and durations of high and low pulses and determines the habitat for aquatic species in the dry and wet seasons (Wang et al., 2016). Flow pulses also provide essential carbon inputs to the riverine ecosystem and strongly support the aquatic food web (Sheldon and Thoms, 2006). Thus, floodplain ecosystems are dependent on naturally dynamic river-flow patterns (Rood et al., 2005). Changes in flow patterns directly affect the floodplain habitats, and thus biodiversity, as exemplified by the reported loss of fish and invertebrates due to dam regulations in the Paraná River basin (Agostinho et al., 2004). Dam impoundments cause salinization and waterlogging which impact the water quality (Tuboí et al., 2017). Similar cases of salinization and waterlogging were reported in the Kabini command area of the Cauvery basin (Nagaraj et al., 2003).

Around 23 per cent of Karnataka's share of Cauvery water is utilized to irrigate highly intensive crops like paddy and sugarcane. Crop productivity and irrigation effectiveness are both impacted negatively by improper cropping patterns over time, which lowers profitability. Similar to this, hydraulic interventions such as dams and barrages changed the Mahanadi River delta from an agrarian system that depended on flooding to a landscape that was vulnerable to flooding (D'Souza, 2006). Since the Hirakud Dam began operating in 1958, the frequency of high floods in the Mahanadi basin has risen from once every 3.48 years to once every 3.3 years (D'Souza, 2006). Furthermore, due to silting of the reservoirs and canals, the tail-end areas do not get adequate irrigation water for the second crop thereby reducing the area for agricultural production (Kulkarni, 2020).

The reported geomorphic consequences of dams include bed armouring, changes in bedform morphology, and sediment depositions downstream that directly affect the channel morphology by narrowing widths, deepening channels and arresting flow within the channel (Pal, 2016; Chong et al., 2021). Downstream bed degradation was accelerated by amplified peak discharges from dams reported in the upper Godavari river basin. (Sanyal et al., 2021). However, no such studies were reported for the Cauvery river basin.

### 5.3. Implications for India

Increasingly empirical data is suggesting that dams, despite large investments, are unable to deliver on their claims (Pradhan and Srinivasan, 2022). The reservoirs are critical for economic growth though it significantly affects the river flow regimes. The costs of dam removals are huge and have both economic and social implications. However, the ill effects of the dams can be minimized by incorporating environmental flows as an integral part of dam development programs. Since irrigation reservoirs have a distinct hydrological influence over hydropower reservoirs, there may be a need to differentiate the e-flow setting based on the purpose of the reservoirs. More research should be done to compare the flow regime changes made by reservoirs serving various purposes to establish e-flow standards that specifically target the impact of that type of reservoir operation. More specifically, in the Cauvery river basin and other related basins where dams are already operational, the reservoir operation rules could be re-calculated to take environmental flow requirements into account, thereby reducing their negative effects.

In India, environmental flows are still not widely acknowledged (Smakhtin and Anupthas, 2006). Even though the Supreme Court of India has mandated a minimum flow of 10 per cent for rivers like Yamuna and Cauvery to improve the water quality (Smakhtin and Anupthas, 2006), the water released from various dams is not well aligned with such environmental flow requirements. There is also a lack of data on the relationships between flows and ecosystem functioning, which impedes the implementation of environmental flow assessment (Jain, 2015). Further, the existing Environmental Impact Assessment (EIA) system in India is unable to keep up with the pace of economic growth and fails to examine and mitigate the broader consequences of widespread dam-building (Erlewein et al., 2013). To improve the EIA, the timing and duration of low/high flow pulses should be considered during the impact assessment of dams in relation to the environmental flows. It can be more effective if the flow requirements for dry and wet years are assessed separately for different reservoir storage levels and reservoir purposes. In addition, the tradeoffs between water security of different stakeholders need to be considered during the design and construction of the dams (Pradhan and Srinivasan, 2022).

## 6. Conclusion

Given the present scenario of changing climate, sustainable water resource management is becoming a bigger issue. Since it is so difficult to integrate natural hydrological processes with reservoir operations, reliable forecasting of future water availability is confronted by significant hurdles. With the proposed modelling approach, the effects of dams on river flow regime can be studied even when no data is available for the period before the dam was constructed. This paper assessed such effects under data-scarce conditions using a landscape-based hydrological model (FLEX-Topo) and Indicators of Hydrological Alterations (IHA) in the upper Cauvery region of India.

The study confirms that the average monthly flow in the upper Cauvery basin is greatly influenced by reservoir operations and subsequent water abstraction in the basin. The decrease in monthly flow is observed across all the sub-basins throughout the year due to reservoir operations when compared to its natural flow regimes. Since irrigation reservoirs have a distinct hydrological influence over hydropower reservoirs, there may be a need to differentiate the e-flow settings based on the purpose of the reservoirs and future research work should be initiated to achieve this target. This can be done, for example, by using the modelling approach presented here to reverse engineer operating rules so flow regimes (such as certain high and low flow percentiles) essential to sustain biodiversity can

be maintained. Further, had there been longer data time series for the inflows and outflows of the reservoirs, better outcomes could have been achieved by the proposed method. The current work also used a simple trigonometric operation rule curve for all the reservoirs. This can be improved further by employing reservoir-specific operation rule curves, which again depend on the availability of appropriate time series data. Nonetheless, the present study presents a way forward to understand the impacts of dams at the basin scale under data-scarce conditions and to help basin managers in formulating strategies to allocate water for both human and environmental needs.

### CRedit authorship contribution statement

**Anjana Ekka:** Methodology, Software, Data curation, Formal analysis, Writing – original draft preparation. **Saket Keshav:** Methodology, Software, Formal analysis. **Saket Pande:** Conceptualization, Supervision, Validation, Writing – review & editing. **Pieter Van der Zaag:** Supervision, Validation, Writing – review & editing. **Yong Jiang:** Supervision, Writing – review & editing.

### Declaration of Competing Interest

The authors declare that they have no known competing financial interests or personal relationships that could have appeared to influence the work reported in this paper.

### Data availability

Data will be made available on request.

### Acknowledgements

This research was financed by the Indian Council of Agricultural Research, Ministry of Agriculture, Government of India through a scholarship for the PhD study [18(26)/2016-EQR/Edn] for the principal author. The authors are thankful to National Data Centre, Central Water Commission, New Delhi for providing gauge station data and GIS-related information on the Cauvery river basin. The authors wish to acknowledge the help provided in this research by the water efficiency task force officers under the India-EU Water Partnership (IEWP). The authors are also thankful to Masoud Amirkhani for providing help with the NSGA algorithm, and Robyn Horon and Chaitanya K.S. for inputs and valuable discussion on the upper Cauvery basin.

### Appendix A. Supporting information

Supplementary data associated with this article can be found in the online version at [doi:10.1016/j.ejrh.2022.101231](https://doi.org/10.1016/j.ejrh.2022.101231).

### References

- Agostinho, A.A., Gomes, L.C., Veríssimo, S., Okada, E.K., 2004. Flood regime, dam regulation and fish in the Upper Paraná River: effects on assemblage attributes, reproduction and recruitment. *Rev. Fish. Biol. Fish.* 14 (1), 11–19. <https://link.springer.com/content/pdf/10.1007/s11160-004-3551-y.pdf>.
- Anderson, E.P., Freeman, M.C., Pringle, C.M., 2006. Ecological consequences of hydropower development in Central America: impacts of small dams and water diversion on neotropical stream fish assemblages. *River Res. Appl.* 22 (4), 397–411. <https://doi.org/10.1002/rra.899>.
- Arthington, A.H., Rolls, R.J., Sternberg, D., Mackay, S.J., James, C.S., 2014. Fish assemblages in subtropical rivers: low-flow hydrology dominates hydro-ecological relationships. *Hydrol. Sci. J.* 59 (3–4), 594–604. <https://doi.org/10.1080/02626667.2013.844345>.
- Babur, M., Babel, M.S., Shrestha, S., Kawasaki, A., Tripathi, N.K., 2016. Assessment of climate change impact on reservoir inflows using multi climate-models under RCPs—The case of Mangal Dam in Pakistan. *Water* 8 (9), 389. <https://doi.org/10.3390/w8090389>.
- Basson, M.S., Allen, R.B., Pegram, G.G.S., & Van Rooyen, J.A., 1994. Probabilistic management of water resource and hydropower systems. Water Resources Publications.
- Beven, K., 2012. Causal models as multiple working hypotheses about environmental processes. *Comptes Rendus Geosci.* 344 (2), 77–88.
- Bhatnagar, D. 2004. Uprooting Forests, Planting Trees: Success of Compensatory Afforestation Measures Mitigating the Deforestation for the Sardar Sarovar Dam, India. University of California at Berkeley, 24. <https://nature.berkeley.edu/classes/es196/projects/2004final/Bhatnagar.pdf>.
- Borgohain, P.L., Phukan, S., Ahuja, D.R., 2019. Downstream channel changes and the likely impacts of flow augmentation by a hydropower project in River Dikrong, India. *Int. J. River Basin Manag.* 17 (1), 25–35. <https://doi.org/10.1080/15715124.2018.1439497>.
- Brauman, K.A., Daily, G.C., Duarte, T.K., Mooney, H.A., 2007. The nature and value of ecosystem services: an overview highlighting hydrologic services. *Annu. Rev. Environ. Resour.* 32, 67–98. <https://doi.org/10.1146/annurev.energy.32.031306.102758>.
- Crook, D.A., Lowe, W.H., Allendorf, F.W., Erős, T., Finn, D.S., Gillanders, B.M., Hadwen, W.L., Harrod, C., Hermoso, V., Jennings, S., Kilada, R.W., 2015. Human effects on ecological connectivity in aquatic ecosystems: integrating scientific approaches to support management and mitigation. *Sci. Total Environ.* 534, 52–64. <https://doi.org/10.1016/j.scitotenv.2015.04.034>.
- Crossman, N.D., Pollino, C.A., 2018. An ecosystem services and Bayesian modelling approach to assess the utility of water resource development in rangelands of north Australia. *J. Arid Environ.* 159, 34–44. <https://doi.org/10.1016/j.jaridenv.2018.02.007>.
- Deb, K., Agrawal, S., Pratap, A., Meyarivan, T., 2000. A Fast Elitist Non-dominated Sorting Genetic Algorithm for Multi-objective Optimization: NSGA-II. In: et al. *Parallel Problem Solving from Nature PPSN VI. PPSN 2000. Lecture Notes in Computer Science*, vol 1917. Springer, Berlin, Heidelberg. [https://doi.org/10.1007/3-540-45356-3\\_83](https://doi.org/10.1007/3-540-45356-3_83).
- Dhanakumar, S., Solaraj, G., Mohanraj, R., 2015. Heavy metal partitioning in sediments and bioaccumulation in commercial fish species of three major reservoirs of river Cauvery delta region, India. *Ecotoxicol. Environ. Saf.* 113, 145–151. <https://doi.org/10.1016/j.ecoenv.2014.11.032>.

- Domingues, R.B., Barbosa, A.B., Sommer, U., Galvão, H.M., 2012. Phytoplankton composition, growth and production in the Guadiana estuary (SW Iberia): Unraveling changes induced after dam construction. *Sci. Total Environ.* 416, 300–313. <https://doi.org/10.1016/j.scitotenv.2011.11.043>.
- D'Souza, R., 2006. *Drowned and Dammed: Colonial Capitalism and Flood Control in Eastern India*. Oxford University Press, New Delhi, India, pp. 1–264. ISBN 0-19-568217-3.
- Efstratiadis, A., Koutsoyiannis, D., 2010. One decade of multi-objective calibration approaches in hydrological modelling: a review. *Hydrol. Sci. J. Des. Sci. Hydrol.* 55 (1), 58–78.
- Erlwein, A., 2013. Disappearing rivers—the limits of environmental assessment for hydropower in India. *Environ. Impact Assess. Rev.* 43, 135–143. <https://doi.org/10.1016/j.eiar.2013.07.002>.
- Fan, Y., Míguez-Macho, G., Jobbágy, E.G., Jackson, R.B., Otero-Casal, C., 2017. Hydrologic regulation of plant rooting depth. *Proc. Natl. Acad. Sci.* 114 (40), 10572–10577. <https://doi.org/10.1073/pnas.1712381114>.
- Fantin-Cruz, L., Pedrollo, O., Girard, P., Zeilhofer, P., Hamilton, S.K., 2015. Effects of a diversion hydropower facility on the hydrological regime of the Correntes River, a tributary to the Pantanal floodplain, Brazil. *J. Hydrol.* 531, 810–820. <https://doi.org/10.3389/jfevs.2020.579031>.
- Gao, B., Li, J., Wang, X., 2018. Analyzing changes in the flow regime of the Yangtze River using the eco-flow metrics and IHA metrics. *Water* 10 (11), 1552. <https://doi.org/10.3390/w10111552>.
- Gao, H., Hrachowitz, M., Fenicia, F., Gharari, S., Savenije, H.H.G., 2014. Testing the realism of a topography-driven model (FLEX-Topo) in the nested catchments of the Upper Heihe, China. *Hydrol. Earth Syst. Sci.* 18, 1895–1915. <https://doi.org/10.5194/hess-18-1895-2014>.
- Gao, H., Hrachowitz, M., Sriwongsitanon, N., Fenicia, F., Gharari, S., Savenije, H.H.G., 2016. Accounting for the influence of vegetation and landscape improves model transferability in a tropical savannah region. *Water Resour. Res.* 52 (10), 7999–8022. <https://doi.org/10.1002/2016WR019574>.
- Gharari, S., Hrachowitz, M., Fenicia, F., Savenije, H.H.G., 2011. Hydrological landscape classification: investigating the performance of HAND based landscape classifications in a central European meso-scale catchment. *Hydrol. Earth Syst. Sci.* 15 (11) <https://doi.org/10.5194/hess-15-3275-2011>.
- Gharari, S., Hrachowitz, M., Fenicia, F., Gao, H., Savenije, H.H.G., 2014. Using expert knowledge to increase realism in environmental system models can dramatically reduce the need for calibration. *Hydrol. Earth Syst. Sci.* 18 (12), 4839–4859. <https://doi.org/10.5194/hess-18-4839-2014>.
- Gierszewski, P.J., Habel, M., Szymańska, J., Luc, M., 2020. Evaluating effects of dam operation on flow regimes and riverbed adaptation to those changes. *Sci. Total Environ.* 710, 136202 <https://doi.org/10.1007/s12665-021-09437-5>.
- Gopal, B., 2016. A conceptual framework for environmental flows assessment based on ecosystem services and their economic valuation. *Ecosyst. Serv.* 21, 53–58. <https://doi.org/10.1016/j.ecoser.2016.07.013>.
- Grill, G., Lehner, B., Thieme, M., Geenen, B., Tickner, D., Antonelli, F., Babu, S., Borrelli, P., Cheng, L., Crochetiere, H., Macedo, H.E., 2019. Mapping the world's free-flowing rivers. *Nature* 569 (7755), 215. <https://doi.org/10.1038/s41586-019-1111-9>.
- Gutierrez, J.C.T., Adamatti, D.S., Bravo, J.M., 2019. A new stopping criterion for multi-objective evolutionary algorithms: application in the calibration of a hydrologic model. *Comput. Geosci.* 23 (6), 1219–1235.
- Han, Z., Long, D., Fang, Y., Hou, A., Hong, Y., 2019. Impacts of climate change and human activities on the flow regime of the dammed Lancang River in Southwest China. *J. Hydrol.* 570, 96–105. [https://ui.adsabs.harvard.edu/link\\_gateway/2019JHyd.570.96H/doi:10.1016/j.jhydrol.2018.12.048](https://ui.adsabs.harvard.edu/link_gateway/2019JHyd.570.96H/doi:10.1016/j.jhydrol.2018.12.048).
- Hargreaves, G.H., Samani, Z.A., 1982. Estimating potential evapotranspiration. *J. Irrig. Drain. Div.* 108 (3), 225–230. <https://doi.org/10.1061/JRCEA4.0001390>.
- Jain, S.K., 2015. Assessment of environmental flow requirements for hydropower projects in India. *Curr. Sci.* 1815–1825. <https://www.curentscience.ac.in/Volumes/108/10/1815.pdf>.
- Janakarajan, S., 2016. The e/Cauvery water dispute: need for a rethink. *Econ. Political Wkly.* 10–15. <https://www.jstor.org/stable/pdf/26270237.pdf>.
- Klingensmith, D., 2003. Building India's 'modern temples': Indians and Americans in the Damodar Valley Corporation 1945–60. *Reg. Mod.: Cult. Polit. Dev. India* 122–142.
- Knighton, A.D., 1988. The impact of the Parangana Dam on the River Mersey, Tasmania. *Geomorphology* 1 (3), 221–237.
- Kulkarni, S., 2020. Canal commands and rising inequity. In: Manisha, R. (Ed.), *Reframing the Environment: Resources, Risk and Resistance in Neoliberal India*. Routledge, India, pp. 141–156.
- Kumar, A.U., Jayakumar, K.V., 2020. Hydrological alterations due to anthropogenic activities in Krishna River Basin, India. *Ecol. Indic.* 108, 105663 <https://doi.org/10.1016/j.ecolind.2019.105663>.
- Li, P., Sheng, M., Yang, D., Tang, L., 2019. Evaluating flood regulation ecosystem services under climate, vegetation and reservoir influences. *Ecol. Indic.* 107, 105642 <https://doi.org/10.1016/j.ecolind.2019.105642>.
- Lu, W., Lei, H., Yang, D., Tang, L., Miao, Q., 2018. Quantifying the impacts of small dam construction on hydrological alterations in the Jiulong River basin of Southeast China. *J. Hydrol.* 567, 382–392. <https://doi.org/10.1016/j.jhydrol.2018.10.034>.
- Mallen-Cooper, M., Zampatti, B.P., 2020. Restoring the ecological integrity of a dryland river: Why low flows in the Barwon–Darling River must flow. *Ecol. Manag. Restor.* 21 (3), 218–228. <https://doi.org/10.1111/emr.12428>.
- Marcinkowski, P., Grygoruk, M., 2017. Long-term downstream effects of a dam on a lowland river flow regime: Case study of the Upper Narew. *Water* 9 (10), 783. <https://doi.org/10.3390/w9100783>.
- Mateo, C.M., Hanasaki, N., Komori, D., Tanaka, K., Kiguchi, M., Champathong, A., Oki, T., 2014. Assessing the impacts of reservoir operation to floodplain inundation by combining hydrological, reservoir management, and hydrodynamic models. *Water Resour. Res.* 50 (9), 7245–7266. <https://doi.org/10.1002/2013WR014845>.
- Mittal, N., Mishra, A., Singh, R., Bhave, A.G., van der Valk, M., 2014. Flow regime alteration due to anthropogenic and climatic changes in the Kangsabati River, India. *Ecohydrol. Hydrobiol.* 14 (3), 182–191. <https://doi.org/10.1016/j.ecohyd.2014.06.002>.
- Mittal, N., Bhave, A.G., Mishra, A., & Singh, R., 2016. Impact of human intervention and climate change on natural flow regime. *Water resources management*, 30(2), 685–699. DOI: 269–015-1185–6. <https://doi.org/10.1007/s11269-015-1185-6>.
- Nagaraj, N., Shankar, K., Chandrakanth, M.G., 2003. Pricing of irrigation water in cauvery basin: case of Kabini Command. *Econ. Political Wkly.* 4518–4520. <https://www.jstor.org/stable/4414182>.
- Ndiritu, J.G. and Sinha, P., 2009, A parsimonious trigonometric model of reservoir operating rules. In International Conference “Water Environment, Energy and Society”(WEES-2009) New Delhi, 12–16 January 2009.
- Nijzink, R.C., Samaniego, L., Mai, J., Kumar, R., Thober, S., Zink, M., Hrachowitz, M., 2016. The importance of topography controlled sub-grid process heterogeneity and semi-quantitative prior constraints in distributed hydrological models. *Hydrol. Earth Syst. Sci.* 20 (3), 1151–1176. <https://doi.org/10.5194/hess-20-1151-2016>.
- O'Sullivan, A.M., Devito, K.J., Curry, R.A., 2019. The influence of landscape characteristics on the spatial variability of river temperatures. *Catena* 177, 70–83. <https://doi.org/10.1016/j.catena.2019.02.006>.
- Page, K., Read, A., Frazier, P., Mount, N., 2005. The effect of altered flow regime on the frequency and duration of bankfull discharge: Murrumbidgee River, Australia. *River Res. Appl.* 21 (5), 567–578.
- Pai, D.S., Sridhar, L., Rajeevan, M., Sreejith, O.P., Satbhai, N.S., Mukhopadhyay, B., 2014. Development of a new high spatial resolution (0.25 × 0.25) long period (1901–2010) daily gridded rainfall data set over India and its comparison with existing data sets over the region. *Mausam* 65 (1), 1–18. <https://doi.org/10.54302/mausam.v65i1.851>.
- Pal, S., 2016. Impact of Massanjore dam on hydro-geomorphological modification of Mayurakshi river, Eastern India. *Environ., Dev., Sustain.* 18 (3), 921–944. <https://doi.org/10.1007/s10668-015-9679-1>.
- Pal, S., Saha, A., Das, T., 2019. Analysis of flow modifications and stress in the Tangon river basin of the Barind tract. *Int. J. River Basin Manag.* 17 (3), 301–321. <https://doi.org/10.1080/15715124.2018.1546714>.
- Pande, S., 2013b. Quantile hydrologic model selection and model structure deficiency assessment: 2. *Appl. Water Resour. Res.* 49 (9), 5658–5673. <https://doi.org/10.1002/wrcr.20422>.
- Pande, S., 2013a. Quantile hydrologic model selection and model structure deficiency assessment: 1. *Theory Water Resour. Res.* 49 (9), 5631–5657. <https://doi.org/10.1002/wrcr.20411>.

- Perkin, J.S., Bonner, T.H., 2011. Long-term changes in flow regime and fish assemblage composition in the Guadalupe and San Marcos rivers of Texas. *River Res. Appl.* 27 (5), 566–579. <https://doi.org/10.1002/rra.1373>.
- Pinder, A.C., Raghavan, R., Britton, J.R., 2015. The legendary hump-backed mahseer Tor sp. of India's River Cauvery: an endemic fish swimming towards extinction? *Endanger. Species Res.* 28 (1), 11–17. (<https://www.int-res.com/articles/esr2015/28/n028p011.pdf>).
- Pradhan, A., Srinivasan, V., 2022. Do dams improve water security in India? A review of post facto assessments. *Water Secur.*, 100112 <https://doi.org/10.1016/j.wasec.2022.100112>.
- Pyron, M., Neumann, K., 2008. Hydrologic alterations in the Wabash River watershed, USA. *River Res. Appl.* 24 (8), 1175–1184. <https://doi.org/10.1002/rra.1155>.
- Raj, B.S., 1941. Dams and fisheries; Mettur and its lessons for India. In *Proceedings of the Indian Academy of Sciences-Section B (Vol. 14, No. 4, pp. 341–358)*. Springer India. <https://www.ias.ac.in/public/Volumes/secb/014/04/0341-0358.pdf>.
- Ramaswamy, R.Iyer, 1994. Indian federalism and water resources. *Int. J. Water Resour. Dev.* 10 (2), 191–202. <https://doi.org/10.1080/07900629408722622>. (<https://doi.org/10.1080/07900629408722622>).
- Rani, S.A.F., Sherine, H.B., 2007. A study on measure of pollution load of well waters in Trichy area. *Indian J. Environ. Prot.* 27 (8), 721–723.
- Renofalt, B.M., Jansson, R., Nilsson, C., 2010. Effects of hydropower generation and opportunities for environmental flow management in Swedish riverine ecosystems. *Freshw. Biol.* 55 (1), 49–67. <https://doi.org/10.1111/j.1365-2427.2009.02241.x>.
- Richter, B., Baumgartner, J., Wigington, R., Braun, D., 1997. How much water does a river need. *Freshw. Biol.* 37 (1), 231–249. <https://doi.org/10.1046/j.1365-2427.1997.00153.x>.
- Richter, B.D., Baumgartner, J.V., Powell, J., Braun, D.P., 1996. A method for assessing hydrologic alteration within ecosystems. In: *Conservation biology*, 10, pp. 1163–1174 <http://doi.wiley.com/10.1046/j.1523-1739.1996.10041163.x>.
- Rood, S.B., Samuelson, G.M., Braatne, J.H., Gourley, C.R., Hughes, F.M., Mahoney, J.M., 2005. Managing river flows to restore floodplain forests. *Front. Ecol. Environ.* 3 (4), 193–201. [https://doi.org/10.1890/1540-9295\(2005\)003\[0193:MRFTRF\]2.0.CO;2](https://doi.org/10.1890/1540-9295(2005)003[0193:MRFTRF]2.0.CO;2).
- Santos, L., Thirel, G., Perrin, C., 2018. Pitfalls in using log-transformed flows within the KGE criterion. *Hydrol. Earth Syst. Sci.* 22 (8), 4583–4591.
- Savenije, H.H.G., 2010. HESS Opinions" Topography driven conceptual modelling (FLEX-Topo)". *Hydrol. Earth Syst. Sci.* 14 (12), 2681–2692. <https://doi.org/10.5194/hess-14-2681-2010>.
- Shah, R.B., 1994. Inter-state river water disputes: A historical review. *Int. J. Water Resour. Dev.* 10 (2), 175–189. <https://doi.org/10.1080/07900629408722621>.
- Sheldon, F., Thoms, M.C., 2006. In-channel geomorphic complexity: The key to the dynamics of organic matter in large dryland rivers. *Geomorphology* 77 (3–4), 270–285. <https://doi.org/10.1016/j.geomorph.2006.01.027>.
- Simões, N.R., Nunes, A.H., Dias, J.D., Lansac-Tóha, F.A., Velho, L.F.M., Bonecker, C.C., 2015. Impact of reservoirs on zooplankton diversity and implications for the conservation of natural aquatic environments. *Hydrobiologia* 758 (1), 3–17.
- Smakhtin, V., Anuphas, M., 2006. An assessment of environmental flow requirements of Indian River Basins. *Int Water Manag. Inst. Res Rep.* 107, 1–42. <https://doi.org/10.3910/2009.106>.
- Smakhtin, V.U., 2001. Estimating continuous monthly baseflow time series and their possible applications in the context of the ecological reserve. *Water Sa* 27 (2), 213–218. <https://doi.org/10.4314/wsa.v27i2.4995>.
- Solaraj, G., Dhanakumar, S., Murthy, K.R., Mohanraj, R., 2010. Water quality in select regions of Cauvery Delta River basin, southern India, with emphasis on monsoonal variation. *Environ. Monit. Assess.* 166 (1), 435–444. <https://doi.org/10.1007/s10661-009-1013-7>.
- Song, X., Zhuang, Y., Wang, X., Li, E., Zhang, Y., Lu, X., Yang, J., Liu, X., 2020. Analysis of Hydrologic Regime Changes Caused by Dams in China. *J. Hydrol. Eng.* 25 (4), 05020003. <https://doi.org/10.3390/w13141961>.
- Srivastava, A.K., Rajeevan, M., Kshirsagar, S.R., 2009. Development of a high resolution daily gridded temperature data set (1969–2005) for the Indian region. *Atmospheric Science Letters* 10 (4), 249–254.
- Sulis, M., Marrocu, M., Paniconi, C., 2009. Conjunctive use of a hydrological model and a multicriteria decision support system for a case study on the Caia catchment, Portugal. *J. Hydrol. Eng.* 14 (2), 141–152. <https://doi.org/10.1061/%28ASCE%291084-0699%282009%2914%3A2%28141%29>.
- Tehrani, M.J., Helfer, F., Jenkins, G., 2021. Impacts of climate change and sea-level rise on catchment management: A multi-model ensemble analysis of the Nerang River catchment, Australia. *Sci. Total Environ.* 777, 146223 <https://doi.org/10.1016/j.scitotenv.2021.146223>.
- Tuboi, C., Irengbam, M. and Hussain, S.A., 2017, Seasonal variations in the water quality of a tropical wetland dominated by floating meadows and its implication for conservation of Ramsar wetlands. *Physics and Chemistry of the Earth, Parts A/B/C*.
- Vaithiyanathan, P., Ramanathan, A.L., Subramanian, V., 1992. Sediment transport in the Cauvery River basin: sediment characteristics and controlling factors. *J. Hydrol.* 139 (1–4), 197–210. [https://doi.org/10.1016/0022-1694\(92\)90202-7](https://doi.org/10.1016/0022-1694(92)90202-7).
- Van Cappellen, P., Maavara, T., 2016. Rivers in the Anthropocene: global scale modifications of riverine nutrient fluxes by damming. *Ecohydrol. Hydrobiol.* 16 (2), 106–111. <https://doi.org/10.1016/j.ecohyd.2016.04.001>.
- Vanham, D., Weingartner, R., Rauch, W., 2011. The Cauvery River basin in Southern India: major challenges and possible solutions in the 21st century. *Water Sci. Technol.* 64 (1), 122–131. <https://doi.org/10.2166/wst.2011.554>.
- do Vasco, A.N., Netto, A.D.O.A., da Silva, M.G., 2019. The influence of dams on ecohydrological conditions in the São Francisco River Basin. *Braz. Ecohydrol. Hydrobiol.* 19 (4), 556–565. <https://doi.org/10.1016/j.ecohyd.2019.03.004>.
- Venkatachalapathy, R., Karthikeyan, P., 2015. Diatom Indices and Water Quality Index of the Cauvery River, India: Implications on the Suitability of Bio-Indicators for Environmental Impact Assessment. *Environmental Management of River Basin Ecosystems*. Springer, Cham, pp. 707–727.
- Wang, G., Xia, J., 2010. Improvement of SWAT 2000 modelling to assess the impact of dams and sluices on streamflow in the Huai River basin of China. *Hydrol. Process.: Int. J.* 24 (11), 1455–1471. <https://doi.org/10.1002/hyp.7606>.
- Wang, Q., Wang, L., Huang, W., Wang, Z., Liu, S., Savić, D.A., 2019. Parameterization of NSGA-II for the optimal design of water distribution systems. *Water* 11 (5), 971. <https://doi.org/10.3390/w11050971>.
- Wang, Y., Rhoads, B.L., Wang, D., 2016. Assessment of the flow regime alterations in the middle reach of the Yangtze River associated with dam construction: potential ecological implications. *Hydrol. Process.* 30 (21), 3949–3966. <https://doi.org/10.1002/hyp.10921>.
- Wheaton, J.M., 2015. *Geomorphic change detection software*. Utah State University.
- Yan, Y., Yang, Z., Liu, Q., Sun, T., 2010. Assessing effects of dam operation on flow regimes in the lower Yellow River. *Environ. Sci. Process* 2, 507–516. <https://doi.org/10.1016/j.proenv.2010.10.055>.